ABSTRACT

Analysis of Fracture System Geometry on the Salt Valley Anticline
Paradox Basin, Utah

Alison L. Nguyen, B.S.

Mentor: Vincent S. Cronin, Ph.D.

The structural geology of the Salt Valley Anticline crest is highly complex. It is erosionally breached by Salt Valley with normal faults and joints as the two dominant brittle structures. The study area is composed of two fault systems and one joint system with three sets of joints. Two major structural events occurred: the formation of the Salt Valley Anticline and its subsequent collapse. Regional extension and consequent salt movement are interpreted to be the underlying causes of the formation of Salt Valley Anticline. Experimental models suggest that regional extension can significantly affect fault patterns on salt domes, much like the patterns found on Salt Valley Anticline. The orientation of the joint sets also supports regional extension as the cause for the Salt Valley Anticline formation.

Analysis of Fracture System Geometry on the Salt Valley Anticline
Paradox Basin, Utah

by

Alison L. Nguyen, B.S.

A Thesis

Approved by the Department of Geology

Steven G. Driese

____
Steven G. Driese, Ph.D., Chairperson

Submitted to the Graduate Faculty of
Baylor University in Partial Fulfillment of the
Requirements for the Degree
of
Master of Science

Approved by the Thesis Committee

Vincent S Cronin

____
Vincent S. Cronin, Ph.D., Chairperson

Rena M. Bonem

____
Rena M. Bonem, Ph.D.

Darrell S Vodopich

____
Darrell S. Vodopich, Ph.D.

Accepted by the Graduate School
December 2006

Larry Lyon

____
J. Larry Lyon, Ph.D., Dean

TABLE OF CONTENTS

LIST OF FIGURES

LIST OF PLATES

ACKNOWLEDGMENTS

When I first began this thesis in 1998, I had no idea it would have taken me so long to finish. Although the thesis was put on the back burner numerous times throughout the years, so that I could do other things with my life such as get married, move into a house, and have a child, I never gave up on the idea of finishing the thesis and graduating one day. My desire and drive to finish this thesis is all due to countless people who have impacted my life in some way. A few of them I shall list and give my gratitude.

I first have to thank Dr. Stacey Atchley, for without his enthusiastic teaching of Historical Geology, I would have never fallen in love with geology.

Secondly, I thank my advisor, Dr. Michael R. Hudec of the Beaurea of Economic Geology, for taking me on as a graduate student and introducing me to Moab, Utah. His faith in my field work, guidance throughout the thesis, and his encouragement for me to finish is appreciated beyond description.

I must extend my deepest gratitude to my thesis chairman, Dr. Vince Cronin, of the Baylor Geology Department. He adopted me as a graduate student when I was in need of help and vowed to get me graduated. I am indebted to him for his tireless work and perseverance.

My second reader, Dr. Rena Bonem, Paulette Penney of the Baylor Geology Department, and Sandra Harman of the graduate school have helped me out so many times I cannot count. They never gave up on me, and for this, I thank them from the bottom of my heart.

My third reader, Dr. Darrell Vodopich of the Baylor Biology Department, deserves my thanks for always being there and willing to help with my thesis.

I also need to thank the geologists at Shell Oil Company, such as, Bert Cox, Mark Picha, Kirk Hansen, and Bill Rizer. Their continued interest in my thesis and encouragement to never give up was much appreciated. Petrophysicists Rich Rosen and Bob Romero, as well as engineer, Gary Beer, also contributed to my desire to finish this thesis.

Above all, I express my sincere gratitude and love to my husband, Mike Nguyen, for never losing faith in me and always pushing me to finish. He has been my rock through it all. He was there with me when I began the field work, with me when I was up all night to meet deadlines, and with me when I decided to finish this for good. He never gave up on me, even when I almost gave up on myself. With his love and support, he helped me see that finishing this thesis was possible and important. If I had given up on this thesis, I would have regretted it for the rest of my life.

CHAPTER ONE

Introduction

The Paradox Basin of Utah, Colorado, New Mexico and Arizona has long drawn the attention of geologists due to the fascinating interplay of tectonics, orogeny, sedimentation, topography and the development of salt-related structures. Petroleum reservoirs associated with salt structures continue to be important exploration targets. The purpose of this study is to document the geometry of fault and joint systems on the Salt Valley Anticline, Paradox Basin, southeast Utah, with particular attention to along-strike variability in their density of occurrence, orientation, and apparent relationship to one another.

The Paradox Basin encompasses approximately 20,000 square miles in Colorado, Utah, Arizona, and New Mexico (fig. 1). It is bordered to the northeast by the Uncompahgre Uplift, to the southeast by the San Luis Uplift, to the south by the Defiance Uplift, and to the west by the Circle Cliffs Uplift, San Rafael Swell, and Monument Upwarp. The Salt Valley Anticline is located in the northwest part of the Paradox Basin fold-and-fault belt. The area where this thesis field study was conducted is located on the crest of the Salt Valley Anticline (fig. 1), in Township 22 and 23 South from the Salt Lake Base Line, and Range 19 and 20 East of the Salt Lake Meridian. The area measures seven miles long by one mile wide, and is part of the area previously mapped by Hellmut Doelling (1994) of the Utah Geological Survey.

Prior to conducting field work, aerial photographs on a 1:25,000 scale were studied with a stereoscope in order to become familiar with the topography and structure of the

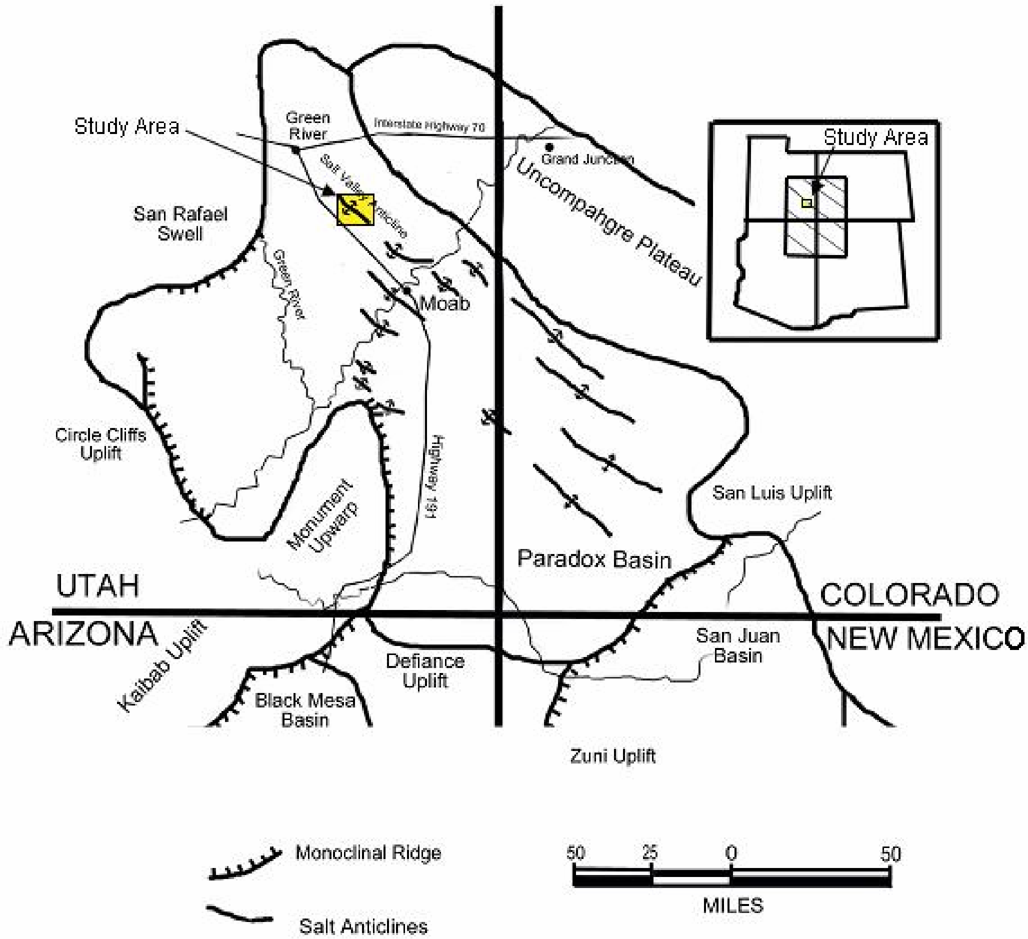

Figure 1. Location map of the Paradox Basin showing the four corners region, the study area (highlighted in yellow), and the major structural elements of the area. Modified from Ohlen and McIntyre (1965) and Molenaar (1981).

area (plate 1). Topographic and geologic maps were also studied to become familiar with the geologic units and the previously mapped structural geology.

The overall map pattern of normal faults in the area was defined by analysis of a mosaic of aerial photographs (plate 1). On aerial photographs, the faults were observed as lineaments characterized by variation in tone or vegetation. Faults interpreted from the aerial photographs were verified during field work, when the faults were examined and measured along their entire lengths. The verification that the photolineaments correspond to faults was typically based on observed structural discontinuities (figs. 2, 3), lithologic discontinuities (fig. 4), and the juxtaposition of strata (fig. 5). Joints were also mapped using the aerial photo mosaic.

The geological units and faults were mapped on mylar overlying the aerial photographs. Wherever possible, fault throw (*i.e.,* the vertical component of the net slip vector) was estimated and recorded in a field book. The strike and dip of both the formations and faults were measured using a Brunton compass. The rake of slickenlines was also measured and recorded.

A detailed surface geologic map was constructed from field data using the ArcGIS computer application (plate 2). Where surface orientations could not be measured in the field, they were computed by solving the corresponding three-point problems. To study the subsurface of the study area, two detailed cross-sections were constructed on a scale of one inch equals 340 feet (figs. 6 and 7).

A.

B.

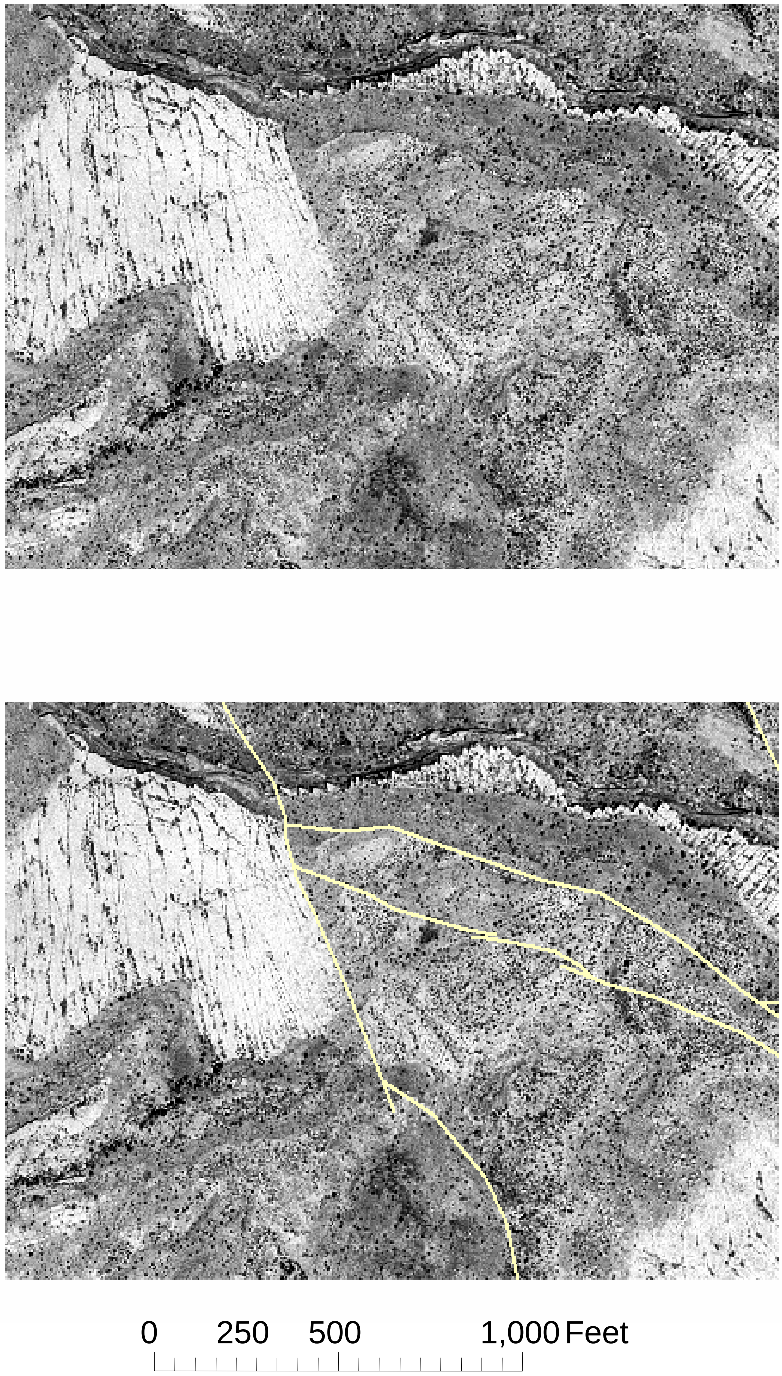

Figure 2. Aerial view of a portion of the study area (A.) showing linear fault traces, and (B.) with yellow lines indicating actual fault locations. Area located in north region of study area.

Figure 3. Photograph of fault scarp that shows structural discontinuity and differential erosion.

Figure 4. Photograph of fault located based on lithologic discontinuity. Fault is indicated with white line. View is toward the northeast of study area.

Figure 5. Photograph showing juxtaposition of strata of the same age (Salt Wash and Tidwell Formations) that represent different sedimentary environments. Photograph was taken in southern part of study area.

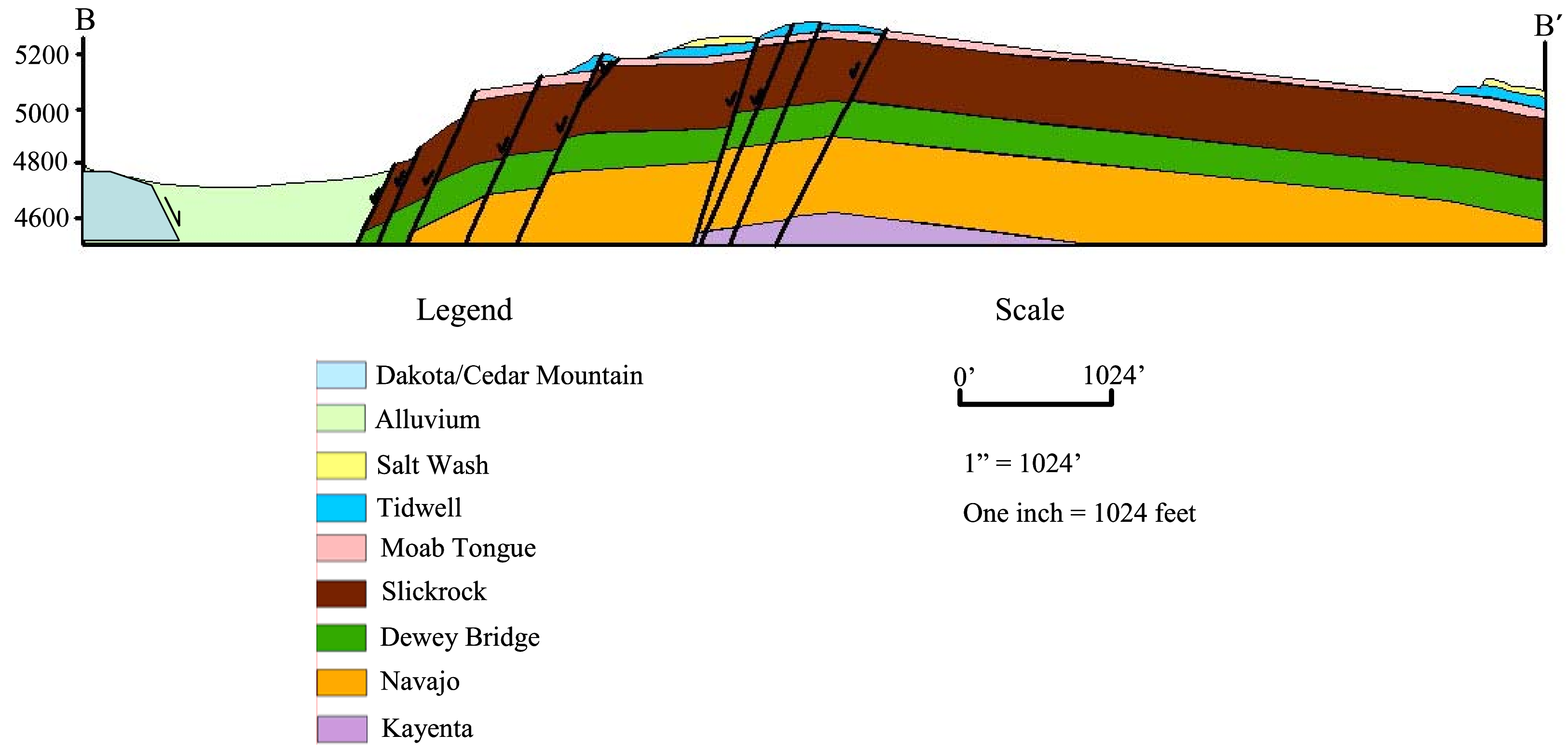

Figure 6. Structurally balanced cross-section A-A’ across the northern end of the area.

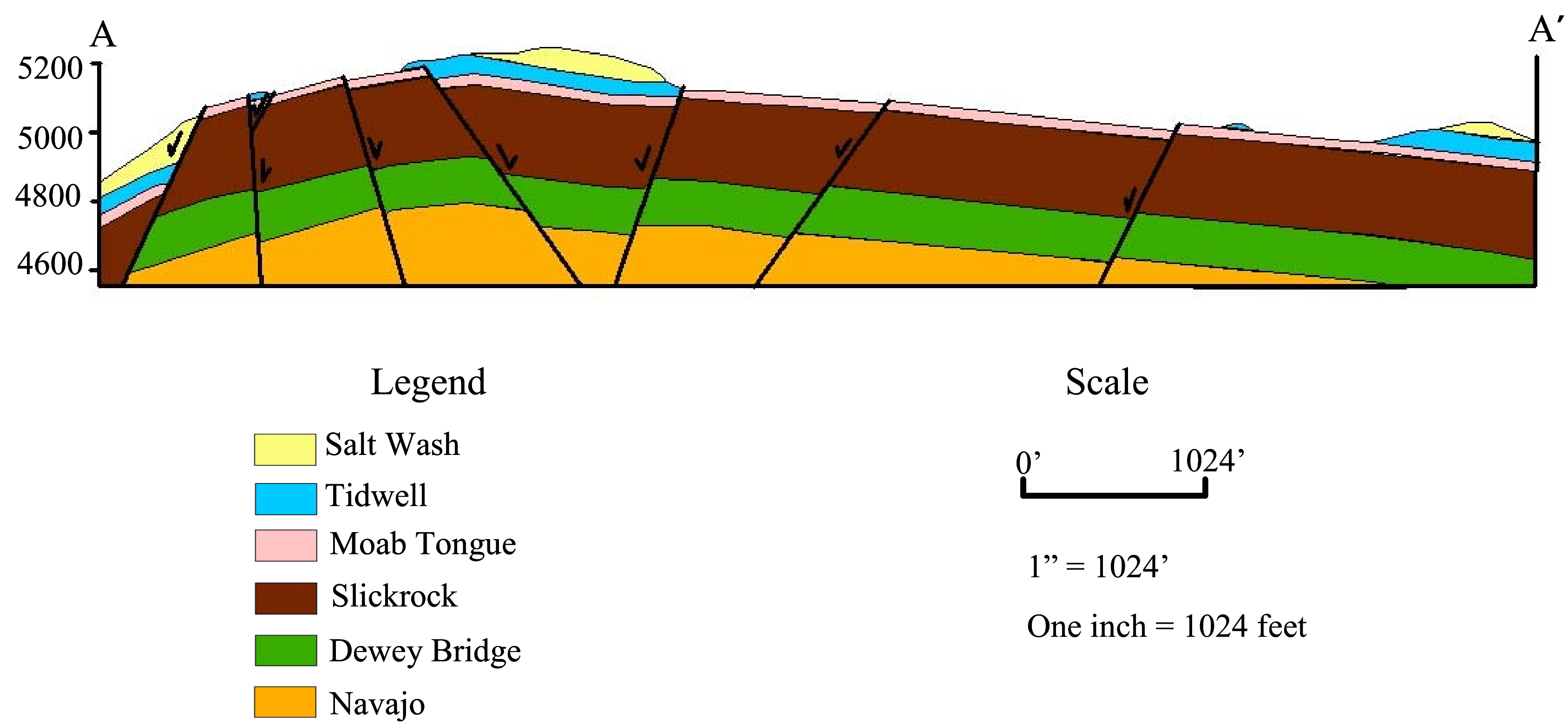

Figure 7. Structurally balanced cross-section B-B’ across the northern end of the area.

CHAPTER TWO

Geologic History

Overview

The Paradox Basin began to form during the growth of the Ancestral Rocky Mountains in the Pennsylvanian. During this orogenic event, several uplifts formed in the area of present-day New Mexico, Colorado, Wyoming, and Utah. The uplift that curves westward into Utah has been named the Uncompahgre Uplift (Stokes, 1986). The rise of the Uncompahgre Uplift was synchronous with subsidence of the adjacent Paradox Basin (Cater and Elston, 1963). Inundation by a shallow sea resulted in salt deposition within the basin (Baars and Stevenson, 1981). Salt movement commenced soon after salt deposition and burial, leading to the development of salt diapirs synchronous with regional extension (Doelling, 1988; Vendeville and Jackson, 1992a). Although the rise of the Uncompahgre Uplift ended in Permian time, salt flow continued well into the Mesozoic. As the diapirs grew, the sedimentary overburden was arched and formed anticlines. Salt movement slowed in the Triassic and ceased by the late Jurassic or early Cretaceous (Baars and Stevenson, 1981). Later regional extension resulted in the collapse of the anticlines.

Paleozoic History

Formation of Ancestral Rocky Mountains

During the Late Mississippian, the eastern and southern margins of North America underwent major orogenic events, resulting in formation of the Ancestral Rocky Mountains in western North America (Budnik, 1986). The Ancestral Rocky Mountains are comprised of approximately 20 basement-involved contractional uplifts and flanking basins that extend from Central Texas to southern Idaho (fig. 8; Barbeau, 2003). The

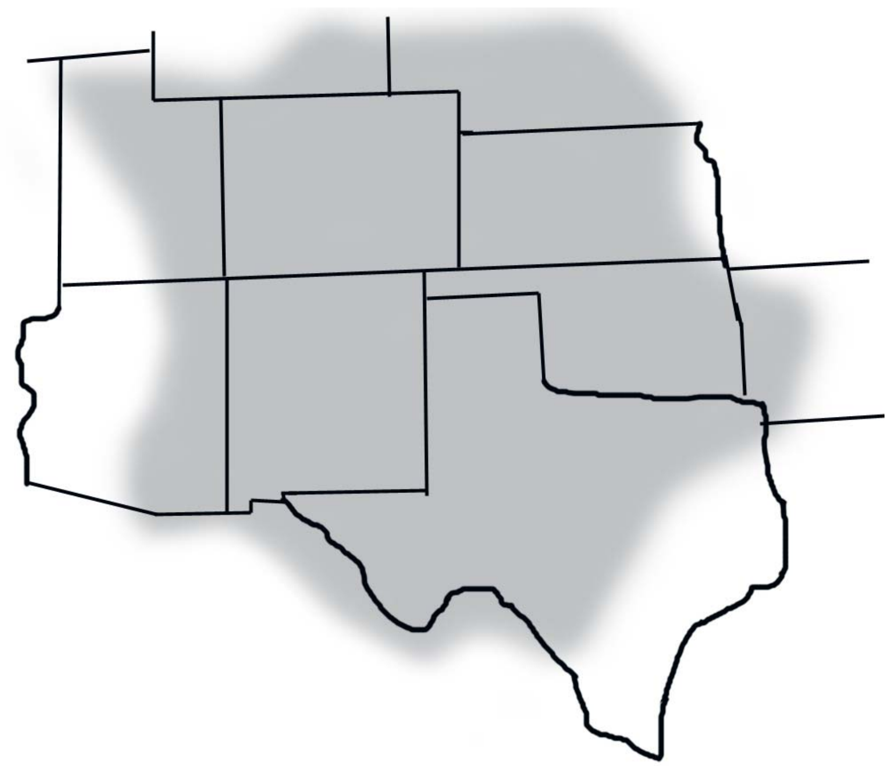

Figure 8. Location of the Ancestral Rocky Mountains, shaded in gray. Modified from Kluth and Coney (1981).

elongate basins trend in a north-to-northwest direction and thicken asymmetrically towards the reverse-fault-bounded uplifts (Ye and others, 1996).

The Ancestral Rocky Mountain orogeny involved a series of deformation pulses that spanned the Mississippian to Early Permian, rather than a single tectonic event. Deformation mainly took place in mid-Pennsylvanian time, with the final phase of deformation occurring in Late Pennsylvannian to Early Permian time (Budnik, 1986). There is a remarkable coincidence in timing and structural style throughout the Ancestral Rocky Mountains, but the plate setting of the paired regions of uplift and basins is unclear because the deformation occupies no discrete belt or domain that relates to contemporaneous plate margins (Ye and others, 1996; Dickinson and Lawton, 2003).

Formation of the Ancestral Rocky Mountains is the most poorly understood tectonic episode in North America's Paleozoic geologic history (Dickinson and Lawton, 2003). Interpretation of the system is difficult since preservation and exposure varies throughout the region and because later deformation has also changed critical relationships. The validity and consistency of interpretations of development must be continually evaluated (Kluth, 1998). There are several models for the development of the Ancestral Rocky Mountains; however, all models are somewhat speculative (Ye and others, 1996).

In one early model, the Ancestral Rocky Mountains were thought to have developed as the result of the North America plate colliding with the South America-African plate (Kluth and Coney, 1981). This model was developed in response to the apparent spatial and temporal coincidence of the Ancestral Rocky Mountains with the Ouachita-Marathon orogenic belt (Ye and others, 1996). The collision of the two plates, which apparently created the Ouachita-Marathon orogen, pushed a peninsular projection of the North

American craton towards the northwest, thus creating the foreland deformation of the Ancestral Rocky Mountains (Kluth and Coney, 1981). This theory is starting to fall out of favor because there are inconsistencies in continental reconstructions, geometries, and stress patterns of this proposed collision (Goldstein, 1981; Warner, 1983).

Another model of development for the Ancestral Rocky Mountains involves regional contraction related to a subduction zone, causing intraplate shortening. Since the subduction boundary is not known from the geologic record, the tectonic style of the margin must be inferred from deformation within the hinterland and its supposed-coeval volcanic arc located in Mexico. Horizontal compressional stresses across this subduction zone would generate the type of shortening in the hinterland that is required to form the reverse fault-bounded basement uplifts (Ye and others, 1996). However, this model is weakened by lack of evidence for the subduction zone, and the volcanic arc in question also postdates the Ancestral Rocky Mountain deformation.

A third, more recent theory as to the cause of development of the Ancestral Rocky Mountains is diachronous subsidence coincident with the closure of the Ouachita suture. As the Ouachita suture belt closed, intracontinental strain was absorbed and reflected in the Ancestral Rocky Mountain deformation. Intracontinental strain declined in intensity near the Ouachita orogenic belt's northwest limit, where structural uplifts were nearly or completely absent (Dickinson and Lawton, 2003).

Rise of the Uncompahgre Uplift and Formation of the Paradox Basin

A set of faults was created or reactivated by the Ancestral Rocky Mountain deformation, thus causing rock surfaces to rise and fall (Elston and Shoemaker, 1960). One of the uplifted blocks of the Ancestral Rocky Mountains, the Uncompahgre Uplift, first appeared in the Pennsylvanian (Stokes, 1986). The Uncompahgre Uplift is a northwest-trending uplift approximately 25-30 miles wide by 95 miles long (Heyman, 1983). The Uncompahgre Uplift is composed of Precambrian crystalline rocks covered by a thin layer of Triassic, Jurassic, and Cretaceous sedimentary rocks (Elston and Shoemaker, 1960). The growth of the uplift was abrupt, rising nearly 15,000 feet in only a few million years (Stokes, 1986). The uplift was likely caused by lateral compression that was also responsible for the subsidence of the flanking basin (Jones, 1959). The Uncompahgre Uplift is bounded by a high angle reverse fault on the southwest, indicated by drilling and seismic data (Frahme and Vauhn, 1983; Hintze, 1988).

As the Uncompahgre Uplift rose, the adjacent Paradox Basin subsided along the uplift's southwest flank (Cater and Elston, 1963; Baars and Stevenson, 1981). Unconformities around the basin's margins indicate this contemporaneous uplift and subsidence. Subsidence began in the Pennsylvanian, indicated by Pennsylvanian nonmarine shales and sandstones (Szabo and Wengerd, 1975). Southwestward thrusting along the Uncompaghre Uplift caused the Paradox Basin to subside, with greatest subsidence located adjacent to the uplift in the northeast (Huffman, 1992; Doelling, 1982). The structural relief between the deepest part of the Paradox Basin and the Uncompahgre Uplift was nearly two kilometers during the Pennsylvanian (Budnick, 1986).

The Paradox Basin, the deepest of any depression in the Ancestral Rocky Mountains, is oval in shape and oriented northwesterly. Its length is 190 miles and its width is 90 miles (Stokes, 1986). Parts of Utah, Arizona, New Mexico, and Colorado are included within the basin, encompassing nearly 20,000 square miles (fig. 1; Szabo and Wengerd, 1975). The Paradox Basin is a flexural basin, developed from southwest-northeast oriented shortening. Proximal areas of the basin cannot be explained by thermal relaxation due to the rapid subsidence; therefore, the Paradox Basin is better explained by the Uncompaghre Uplift's supracrustal loading resulting in flexing of the lithosphere (Barbeau, 2003).

Salt Deposition

Within the Ancestral Rocky Mountains, the Paradox Basin is regarded as unique because of the large quantities of salt deposited within the basin (Hintze, 1988). The salt beds of the Paradox Basin are the thickest in the United States (Wengerd and Strickland, 1954). The salt was deposited because the Paradox Basin was flooded by an advancing sea. Continued subsidence and sedimentation resulted in development of a sabkha depositional environment (Hintze, 1988). The warm climate caused sea water to evaporate, resulting in salt deposition (Doelling, 1985). A total of 29 separate cycles of evaporates characterizes the Paradox Formation found within the basin (Elston and Shoemaker, 1962). The salt thickens against the adjacent Uncompahgre Uplift (fig. 9).

The depositional thickness of the salt is believed to have been approximately 5,000 to 7,000 feet; however, it is difficult to estimate because of later salt flowage (Stokes, 1986).

The presence of immature arkosic debris in the Paradox Basin indicates that the Uncompaghre Uplift had a pulse of uplift in Late Paleozoic time, most likely terminating the conditions requisite for the deposition of the salt. The Paradox Basin might have

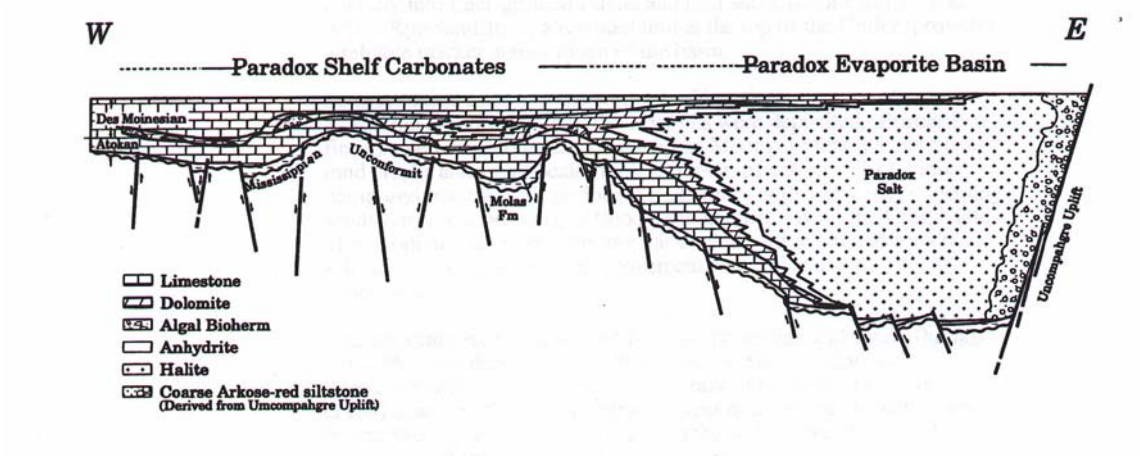

Figure 9. Diagrammatic cross-section of the Paradox Basin and Uncompahgre Uplift. From Baars and Stevenson, (1981).

undergone regional southwest tilting at the same time, also contributing to the cessation of salt deposition.

Rise of Salt Diapirs

Soon after the salt was deposited, it began to flow and form salt diapirs. The Paleozoic and Mesozoic stratigraphy and structure flanking the diapirs indicates salt upwelling in the cores and salt withdrawal from peripheral areas (Elston and Shoemaker, 1962). Salt is a viscous medium with very low strength in the subsurface that flows in response to a differential stress. There are different models to explain the development of this differential stress, including movement on basement faults, differential loading, and regional extension.

The earliest models in the basin favored differential loading as the cause for diapirism (Baars, 1966; Jones, 1959). A viscous material such as salt will flow from an area of higher pressure to an area of lower pressure (Jones, 1959). The eroding Uncompahgre Uplift shed more than 8,000 feet of sediment into the basin on top of the salt during the

Permian, creating enough stress by differential loading to move the salt. As the salt moved, it was deflected upward against basement fault blocks, thereby forming diapirs (Baars, 1966).

Although differential loading is a plausible reason for diapirism, regional extension may also have played a role (fig. 10). Sandbox models have shown that grabens formed above the diapirs are commonly a result of regional extension. Vendeville and Jackson

Figure 10. Cross section depicting some fault structures that may result from regional extension with a lower salt layer (cross pattern). Modified from Ge and others (1994).

(1992b) conducted a series of experiments where a brittle, sand overburden was mechanically extended above a viscous material resembling salt. When extension first occurred, two normal faults with opposite dips formed a graben (fig. 9; Vendeville and Jackson, 1992b). As extension continued, a new fault formed inside the graben paralleling one of the boundary faults (Vendeville and Jackson, 1992a). The viscous salt began upwelling in the footwall of this fault, located in the center of the graben. The upwelling was not a response of forceful intrusion, but a result of a simple fluid pressure gradient and possible differential loading. With further extension, numerous similar faults formed progressively in the axis of the graben (Vendeville and Jackson, 1992b). The viscous material continued to rise where the overburden was thinnest, thus forming a triangular-shaped diapir.

Eventually, the overburden thins by extension creating multiple faults to the point where the strength of the overburden is easily pierced by the growing diapir. Fluid pressure drives the diapir to break through the thinned overburden roof. At the point of intrusion, the diapir changes from reactive to active (fig. 11c). In active diapirism, the growth is no longer controlled by regional extension, but by local stresses (Vendeville and Jackson, 1992a).

A third stage of diapirism, passive diapirism, occurs when the diapir reaches the surface (fig. 11e). Passive diapirs grow during sedimentation, rising fast enough to remain at the surface. All three stages of diapirism, reactive, active, and passive, are required in order for the salt diapir to rise and pierce the overburden.

Once the salt was deposited in the Paradox Basin, it went through the reactive, active, and passive stages (fig. 12). By the end of the Pennsylvanian, the diapirism was in the reactive stage with salt upwelling due to fluid pressure and differential loading of the overburden. As the Permian came to a close, the Paradox Basin diapirs pierced the thinned overburden and were in the active stage. By the Early Cretaceous, the diapirs reached the surface and continued to grow in the passive stage.

Mesozoic History

Triassic Deposition

At the beginning of the Triassic period, tidal flats and flood plains spanned the area, on which were deposited fine sands and silts. As the seas retreated westward, sandstones were deposited. They were most likely deposited by a combination of river systems and wind on wide coastal areas.

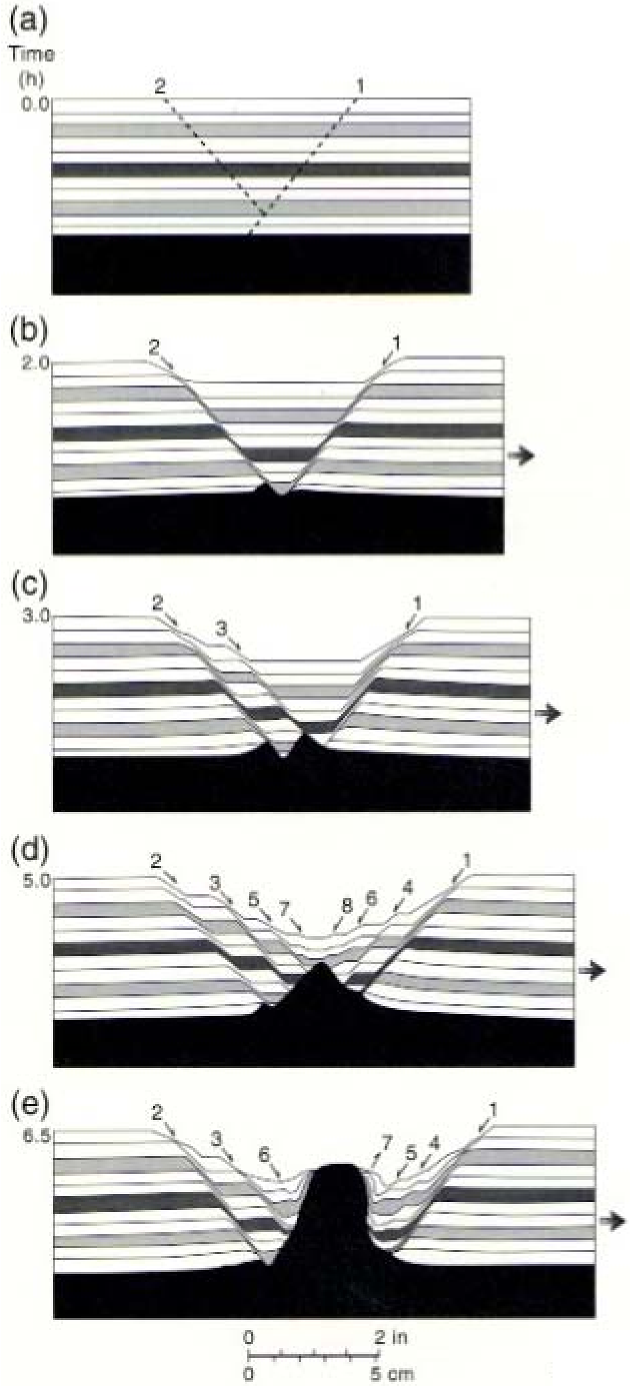

Figure 11. Experimental model showing graben formation and salt diapir rise. From Jackson and Vendeville (1994).

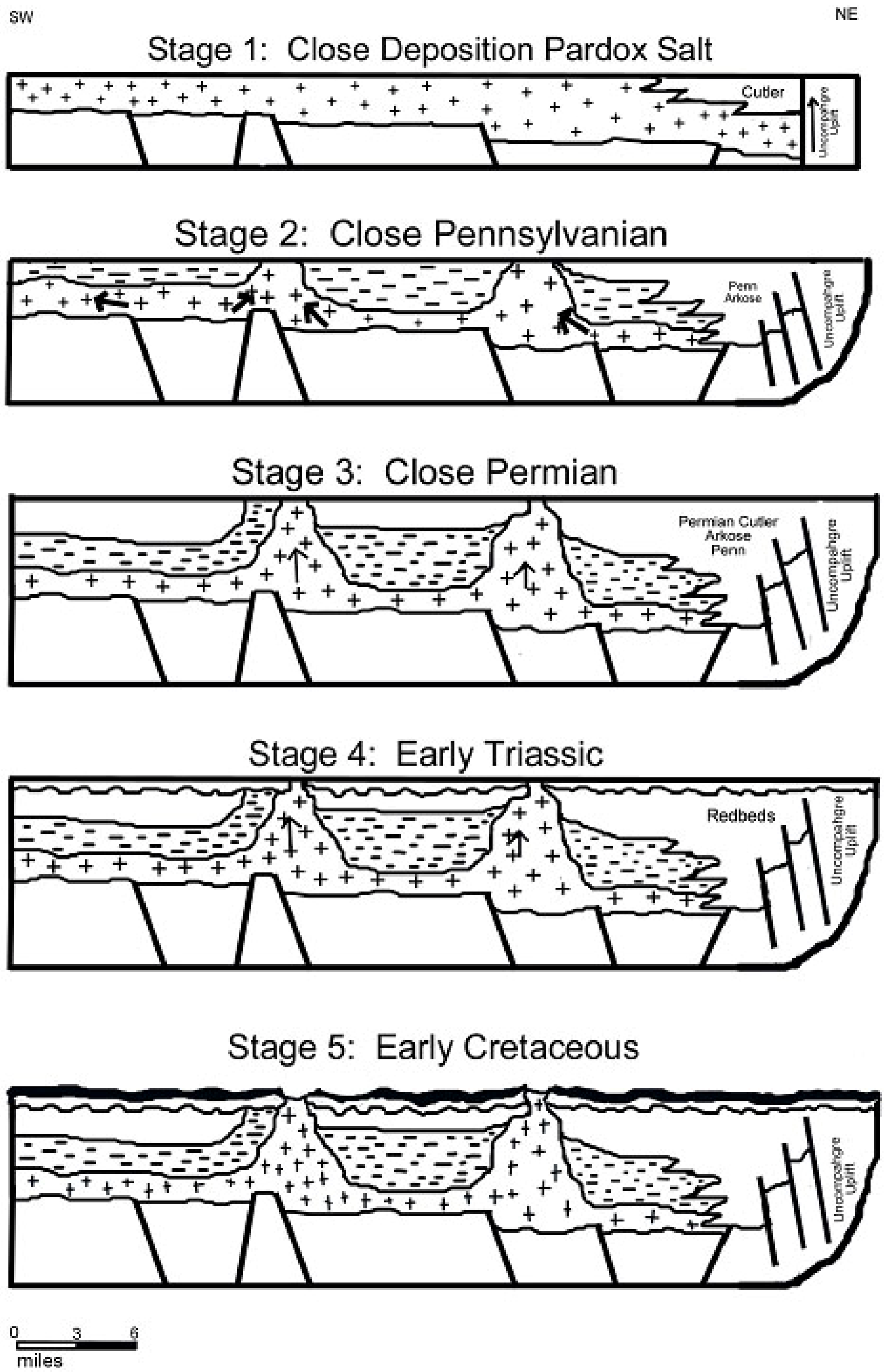

Figure 12. Stages of salt tectonics in the Paradox Basin. Vertical exaggeration is 2x. Modified from Ohlen and McIntyre (1965).

Salt movement continued to affect the deposition and thickness of sediment (Doelling, 1985). By middle Triassic, most of the salt diapirs had been buried by sediments, with few local salt ruptures present (Ohlen and McIntyre, 1965). The growth rate of the salt diapirs was correlated with the subsidence rate of the Paradox Basin. When local subsidence of the basin had ceased in middle Triassic time, the growth of the diapirs slowed considerably (Elston and Shoemaker, 1962).

Jurassic Deposition

During the first part of Jurassic time, a sea inundated central Utah and deposited sediments representative of tidal flats and beaches. The sea retreated again, and the sediments deposited during Jurassic time were characteristic of stream channel and broad flood plain deposits.

Cretaceous Deposition

During Late Cretaceous time, another sea transgressed into central Utah and deposited sediments along the coastal regions, as well as depositing approximately 3,000 feet of gray mud that covered virtually everything in the area. The Mancos Sea retreated approximately 80 million years ago, marked by the deposit of sediments indicative of beach environments, then coastal plain environments, followed by fluvial and lake depositional environments (Doelling, 1985).

The diapirs had continuous growth from the early Permian until the Cretaceous, indicated by Triassic and Jurassic formations thinning over the salt structures (fig. 12; Jones, 1959). The salt's rate of upwelling either balanced or slightly exceeded its rate of removal at the surface (Cater, 1960). The ultimate cessation of the growth of the salt walls occurred in late Mesozoic time and was due to the exhaustion of salt beneath the flanks of the salt walls (Elston and Shoemaker, 1962).

Cenozoic History

Anticline Formation

The structural features most interesting of the Paradox Basin are found in the Paradox fold-and-fault belt, adjacent to the Uncompahgre Uplift's southern flank (fig. 13). This belt is characterized by faulted anticlines over the tops of the diapirs (Szabo and Wengerd, 1975). The cause of these anticlines is currently a matter of debate. In early Tertiary time, the rocks overlying the diapirs were folded either due to regional compression or regional extension that produced additional uplift of the Uncompahgre highland (Elston and Shoemaker, 1962). As the diapirs rose, the sedimentary overburden was arched over each diapir, subsequently forming fifteen salt anticlines in the region (Doelling, 1983). The salt anticline area is approximately 100 miles long and 30 miles wide (Elston, 1960). The anticlines trend northwest and parallel the Uncompahgre front, which closely follows the ancestral Uncompahgre Uplift (Cater, 1960). The anticlines that are further away from the ancestral Uncompahgre Uplift show less intense deformation than the anticlines close to the ancient front (Elston and Shoemaker, 1962).

Anticline formation has been attributed to horizontal contraction or shortening. However, structural features found on the crests of the anticlines have recently been linked to regional extension, much like the rise of salt diapirs (Ge and others, 1996). Characteristic structural features of regional shortening are not found on the crests,

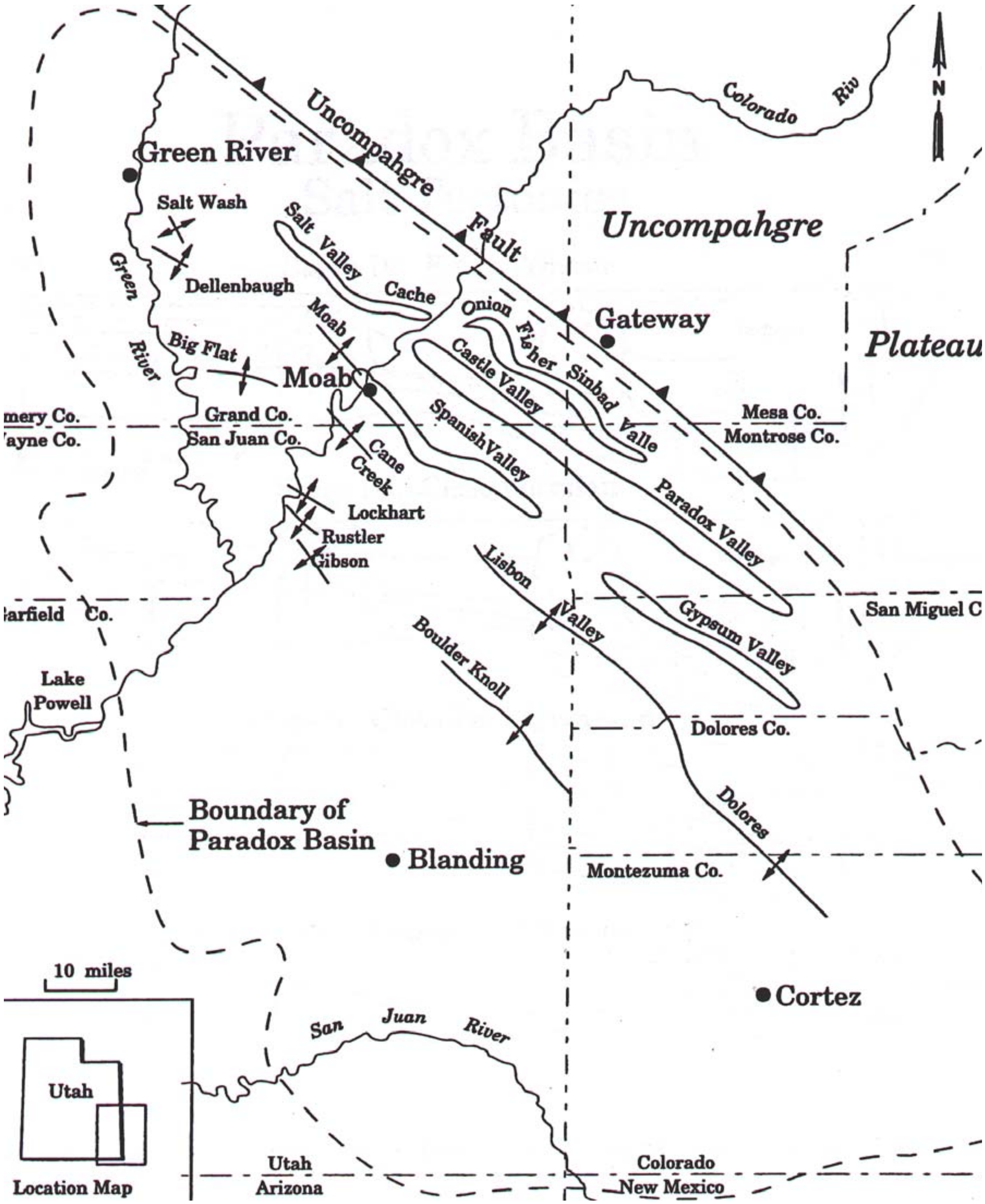

Figure 13. Major salt structures found within the Paradox fold-and-fault belt. Modified from Doelling (1985).

whereas features of regional extension are abundant. Experimental results by Ge and others (1996) were similar to the diapir-growth experiments by Vendeville and Jackson (1992a). The experiments indicated that the diapir rose below a crestal graben, therefore causing later sedimentation to gently fold over the intruded salt diapir.

As the roofs of the salt walls were folded into anticlines, faulting occurred (Ohlen and McIntyre, 1965). These faults mostly developed where the rocks were weakest, along the anticline flanks. Along with the faults, prominent joints formed due to the Tertiary folding (fig. 14; Doelling, 1988).

Anticline Collapse

The anticlines collapsed in the late Tertiary along their crests, forming a steep-walled erosional valley called Salt Valley (fig. 15; Woodward-Clyde, 1983; Elston and Shoemaker, 1962). The collapse has added greatly to the anticlines' structural complexity. Resulting features of collapse include faults, slump features, down-dropped blocks, and down-warped areas (Cater, 1960). There are two potential explanations for the collapse of the anticlines: dissolution and extension. Characteristics of both can be found in the collapsed crests of the anticlines.

The most common model for collapse involves dissolution of the salt. This is the typical way of eroding salt anticlines. Dissolution of the salt occurs when non-saline groundwater reaches the salt through joints or faults and creates solution cavities, thereby allowing the overlying strata to collapse into the voids (fig. 16; Doelling, 1988).
In the Late Tertiary, the Colorado Plateau rose above the surrounding landscape, producing deep canyons and exposing the underlying salt to groundwater (Woodward-

A.

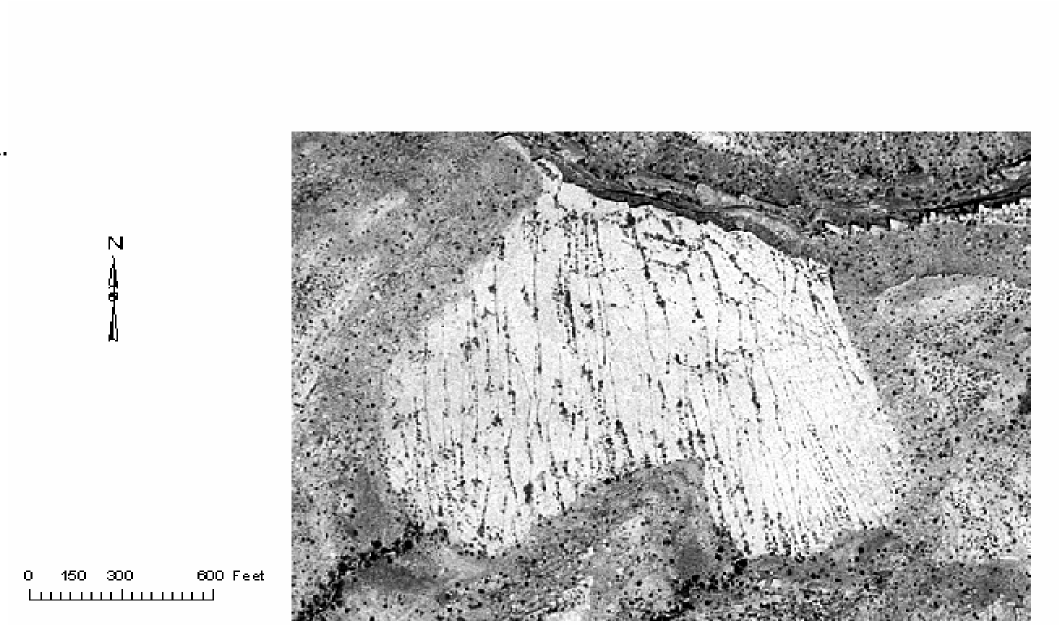

B.

Figure 14. Most joints observable in aerial photography (A) appear to be continuous across the outcrop. When observed in the field (B), smaller secondary joints and discontinuous members of the dominant joint set are more apparent. Photograph taken in southern region of the study area with a view toward northeast.

A.

B.

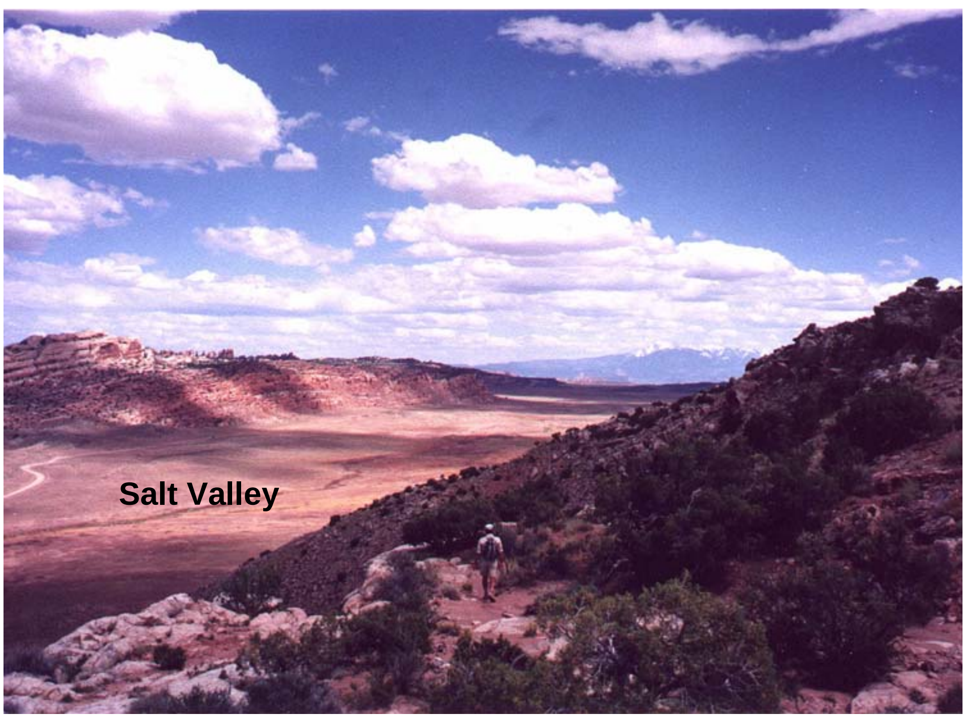

Figure 15. View of Salt Valley from near the crest of Salt Valley Anticline (A) toward the north and (B) toward the south.

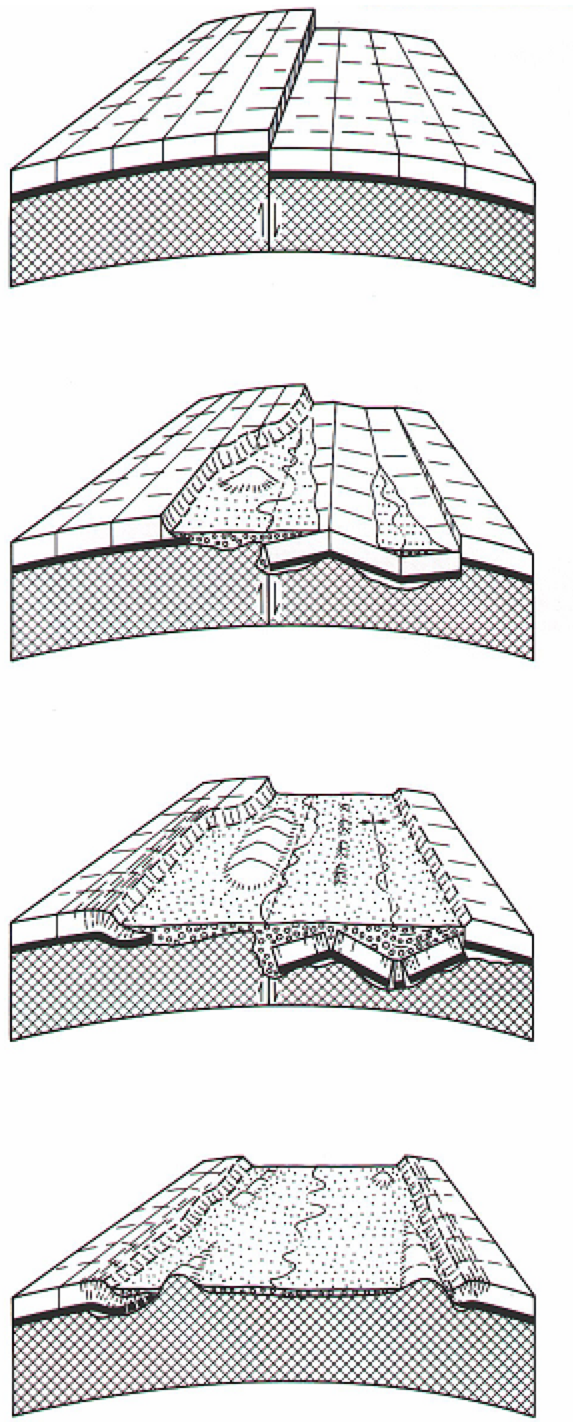

Figure 16. Diagrammatic process of dissolution collapse. From Doelling (1985).

Clyde, 1983). The entrenchment of streams was a result of the uplifted Colorado Plateau. The region's principle streams transect several salt anticlines (Elston and Shoemaker, 1962). The deepest crestal collapse has been noted to occur along the principal drainages in the area (Doelling, 1982). Dissolution of salt most likely occurred during this period since the salt core was exposed to weathering (Doelling, 1988; Stokes, 1986). As the collapse of the anticline deepened, some of the fractures in the area became faults (Doelling, 1982).

The other model for anticline collapse is regional extension (fig. 17). Structural patterns above the anticlines are consistent with field observations and experimental tests of extensional terrains. En echelon normal fault patterns on the crest of the anticlines and faults deflecting off of Salt Valley's northwest end suggest north-to-northeast directed regional extension (Ge and others, 1994).

As regional extension continued, passive diapirs rose until the salt source was exhausted. At this point, the diapir was stretched and a graben formed on the crest. Extension caused the diapir to fall along the faults of the graben leaving residual salt cusps along the faults (fig. 17d). The presence of these cusps indicates that dissolution could not have been the major cause for collapse because dissolution would not have left salt cusps.

Experimentation has shown that dissolution creates distinctive structural systems with normal faults. However, these faults are balanced by reverse faults and folds, which are not found in large enough quantities on the crests of the anticlines to support dissolution as the main cause a cause for anticline collapse. Although the extensional model argues against dissolution as the main avenue for anticline collapse, it does not argue against local dissolution acting in combination with the extension (Ge and others, 1996). Salt dissolution is interpreted to be only a minor influence on the faulting above the anticline crests (Ge and others, 1994).

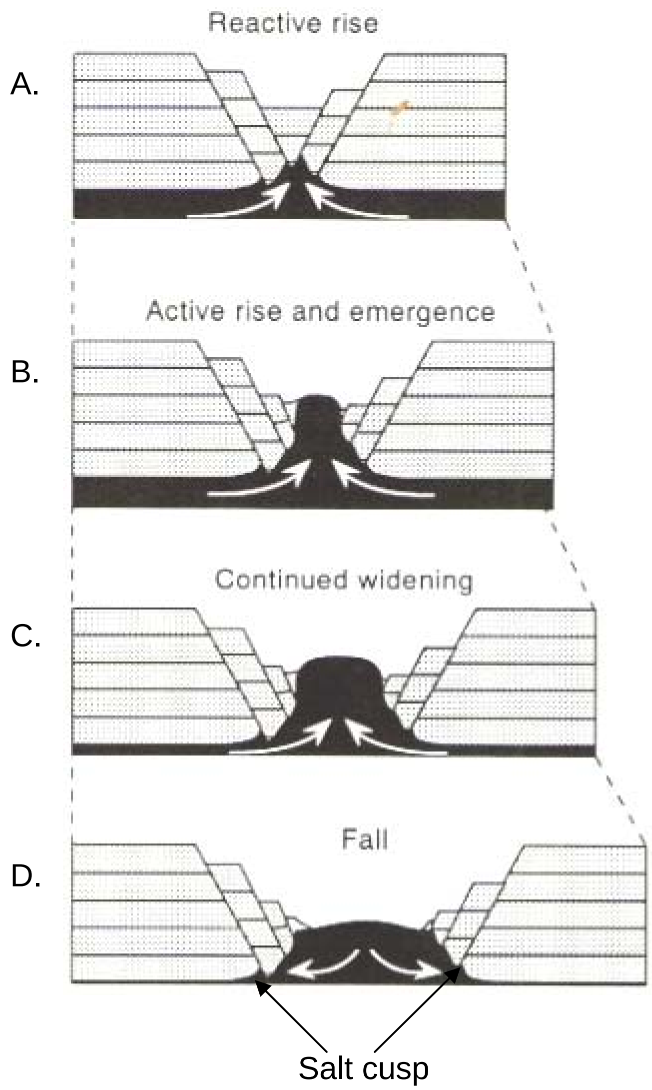

Figure 17. Schematic diagram of extension resulting in eventual diapir collapse. From Vendeville and Jackson (1992b).

CHAPTER THREE

Stratigraphy

Overview

Excellent exposures of the diapir roof are present in the area of the Salt Valley Anticline. Exposed rocks lie above Precambrian-Mississippian shelf strata and range in age from Pennsylvanian to Cretaceous (fig. 18; Doelling, 1982). The Lower Pennsylvanian Paradox Formation includes the thick salt deposits. Upper Pennsylvanian through Triassic deposition is predominantly the Paradox Basin conglomeratic fill, and Jurassic and Cretaceous sandstones, shales and limestones subsequently covered the entire southwest United States.

Jurassic Stratigraphy

The Jurassic units are among the most scenic in Utah. There are three main categories of Jurassic rocks: Early Jurassic non-marine sandstones, Middle Jurassic rocks noted by changing conditions due to an advancing and retreating epicontinental sea, and non-marine Late Jurassic rocks replete with streams and lakes (Hintze, 1988).

Navajo Formation

The Navajo Formation is an aeolian sandstone that conformably overlies the Kayenta Formation, except at the northwest end of Salt Valley Anticline where the Conoco #1 Salt Valley well has shown that only 178 feet of Navajo was intercepted before reaching the Paradox Formation (fig. 19; Doelling, 1988). It consists of pale orange to light gray

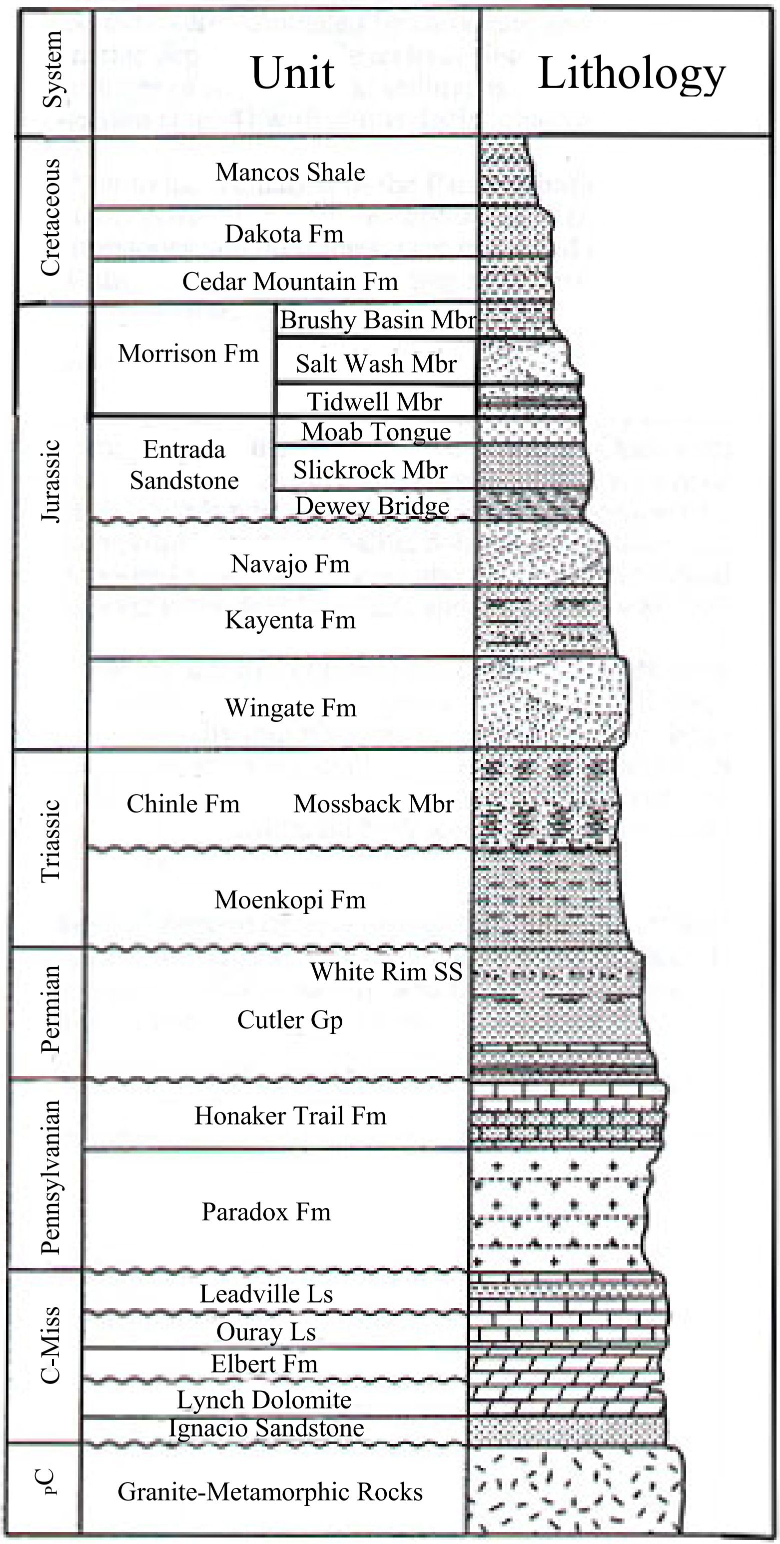

Figure 18. Generalized regional stratigraphic column for the Paradox Basin.

Figure 19. Navajo Formation located at the northwest end of Salt Valley Anticline .

sandstone with sparse blue-gray limestone beds within the formation. These sporadic, lenticular limestones are thought to be of a lacustrine (playa lake) origin and are found on the flanks of Salt Valley Anticline, most notably on the southwest flank (Doelling, 1988; Molenaar, 1981). The Navajo Formation is fine-grained, well sorted, and contains well rounded sand grains and large-scale dune cross-beds suggesting wind-blown sands. The cross-beds dip mainly to the southeast, thus indicating winds from the northwest (Molenaar, 1981). Vertical cliffs form in the lower parts of the Navajo Formation and domes and rounded slopes form in the upper parts.

The Navajo Formation regionally thins west to east across Salt Valley Anticline and has been modified in thickness locally by salt movement. The thickness ranges from 250 to 360 feet where it was influenced by salt movement and from 300 to 450 feet where salt movement did not have an influence (Doelling, 1988). The thickness is 285 feet in the study area (Doelling, 1981).

Entrada Formation

The Entrada Formation consists of three members: the Dewey Bridge Member, the Slick Rock Member, and the Moab Tongue Member (fig. 20). All three members are

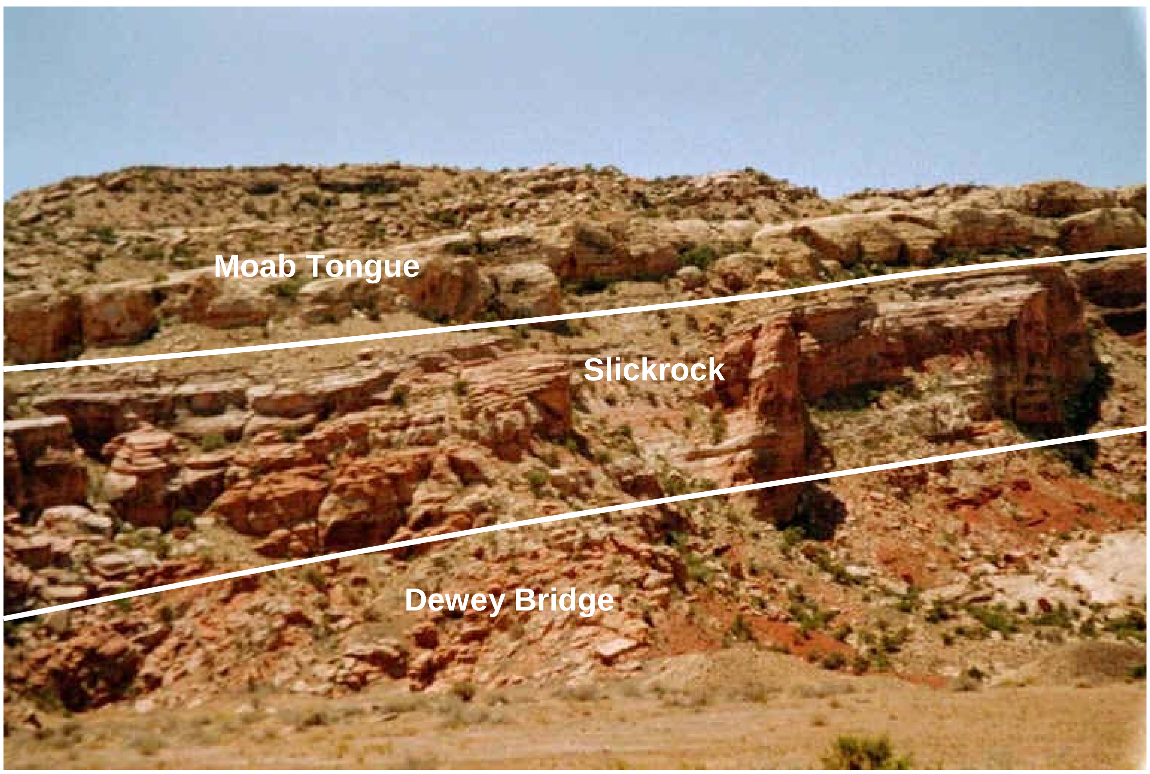

Figure 20. Dewey Bridge, Slickrock, and Moab Tongue Members of the Entrada Formation.

non-marine sandstones and form prominent cliffs (Ohlen and McIntyre, 1965). Some members of the Entrada Sandstone, such as the Slickrock and Dewey Bridge Members, are more easily weathered because of their poor cementation, and form slopes in certain areas.

The cliffs developed in these members are easily dissolved by meteoric water due to their calcareous cementation. All the members thicken regionally to the west, with considerable thickness variation across the study area ranging from 100 feet to 755 feet (Doelling, 1988). This variation is due to syndepositional salt movement. As the anticline formed, new sedimentary layers thinned over the crest of the structure and filled up the subsiding troughs (Doelling, 1985).

Dewey Bridge Member. The Dewey Bridge Member is located at the base of the Entrada Formation and unconformably overlies the Navajo Formation (fig. 20; Molenaar, 1981). It has been known as the Carmel Formation, but a facies change from siltstone to sandstone near the Green River made it useful to apply a different formation name. This mostly fine-grained reddish-brown sandstone weathers to thin, rounded ledges with thicknesses of one to two feet. Siltstone interbeds occur throughout the entire member. The bedding of the Dewey Bridge Member is irregular and highly contorted; however, the formation does not appear to show signs of deformation related to salt movement (Doelling, 1988). Dane (1935) interpreted the contorted bed formation as being due to differential loading of the thick eolian sands of the upper Entrada Formation upon the unconsolidated, water-saturated Dewey Bridge Member (Molenaar, 1981). Because of its muddy sandstone composition, the deposition of the Dewey Bridge Member was most likely on broad tidal flats, which were located marginal to a sea.

The entire thickness of the Dewey Bridge Member ranges from 20 to 175 feet regionally (Doelling, 1988). The thickness in the study area is approximately 125 feet (Doelling, 1981).

Slickrock Member. The Slickrock Member of the Entrada Formation is a massive sandstone that overlies the Dewey Bridge Member conformably and weathers to form cliffs and rock slopes (fig. 20; Molenaar, 1981; Doelling, 1988). The unit is very fine to fine-grained, and generally uniform in its reddish-orange to dark brown color. In some areas, the Slickrock Member is striped or banded, as in the northwest portion of Salt Valley Anticline (Doeling, 1988). Two depositional environments are expressed in the rocks of the Slickrock Member. Large-scale cross beds indicate an aeolian origin, while the horizontal bedding zones are indicative of a shallow marine environment (Molenaar, 1981). The Slickrock Member was most likely deposited marginal to a western sea (Doelling, 1988). From the angle of the cross stratification, northeast or east winds dominated the depositional environment (Molenaar, 1981).

Regional thicknesses of the Slickrock Member range from zero to 400 feet, and a three-point calculation in the study area with location Township 22S and Range 19E, yields a thickness of 245 feet. The unit may, however, thin over the crest of the Salt Valley Anticline (Doelling, 1988).

Moab Tongue Member. The uppermost member of the Entrada Formation is the Moab Tongue Member (fig. 20). Its basal contact with the Slickrock Member is a sharp, angular unconformity or horizontal bedding plane that formed most likely in response to salt flowage (Molenaar, 1981). An unconformity also exists at the top of the Moab

Tongue Member above the Salt Valley Anticline (Doelling, 1988). The color of the Moab Tongue Member is pale orange to beige and white, except at the basal contact, which is marked by a thin, purple-red shale layer (Molenaar, 1981). This fine to medium grained cliff-forming sandstone is observed along intensely jointed dip slopes on either side of Salt Valley Anticline (fig. 21; Doelling, 1988). Primary structures found in the area are low-angle cross

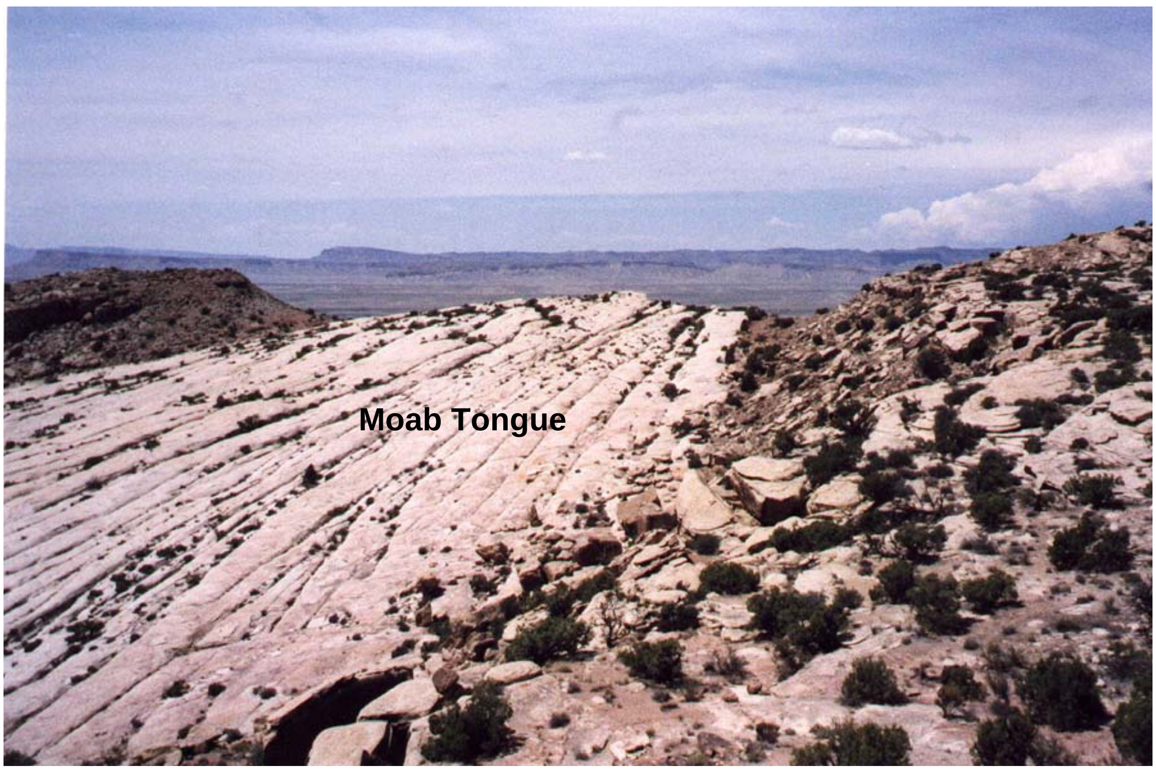

Figure 21. Moab Tongue Member of the Entrada Formation showing highly jointed flat slab.

stratification, which indicates that the most likely depositional environment was a coastal dune complex (Molenaar, 1981; Doelling, 1988).

The thickness of the Moab Tongue Member ranges from 10 to 60 feet regionally and is 35 feet in the study area, based on a three-point calculation at a site in Township 22S and Range 19E.

Morrison Formation

The Morrison Formation of Late Jurassic age is comprised of three members: the Tidwell Member, the Salt Wash Member, and the Brushy Basin Member. Each is very well exposed in the outer flank of Salt Valley (Doelling, 1988). Because the Morrison Formation was deposited in a dry climate with seasonal flooding, many different lithologies are present. The dominant lithology is sandstone, but limestone beds are present in the Tidwell Member. Shales and silts are also commonly found within the Morrison Formation. Volcanic ash found in the upper part of the formation suggests tectonic activity and increased volcanism (Craig and Cadigan, 1958). All three members are slope-forming and tend to erode easily (Doelling, 1988).

Tidwell Member. The Tidwell Member has previously been mapped as the Summerville Formation. The unconformity that exists at the top of the Moab Tongue Member is the same unconformity that has been noted to the west in the San Rafael Swell above the Summerville Formation. Thus, the Moab Tongue Member correlates with the Summerville Formation rather than the Tidwell Member. The Tidwell Member unconformably overlies the Moab Tongue Member (fig. 22).

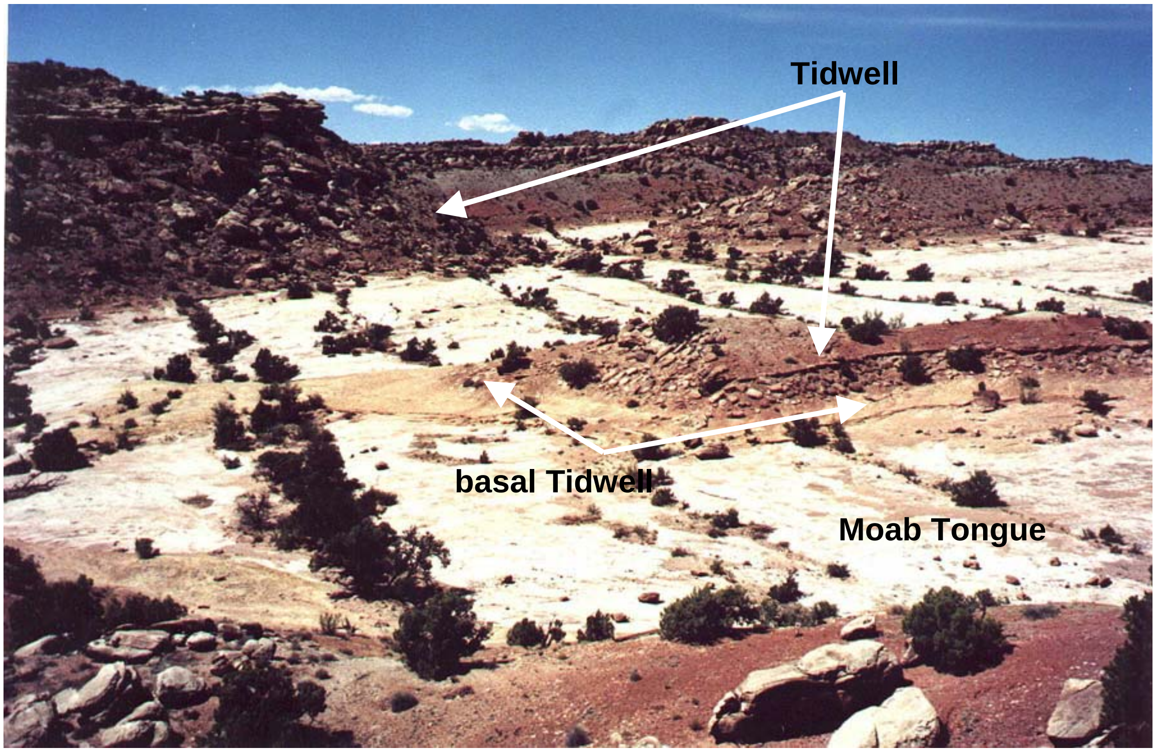

Figure 22. Tidwell Member of the Entrada Formation. The basal contact of the Tidwell with the Moab Tongue is exposed.

Three lithologies comprise the Tidwell Member: sandstone, shale, and limestone. It weathers to form steep, earthy slopes readily and thus, little bedding is displayed. The medium-grained sandstone is interbedded with shale, and limestone appears in ledges with chert concretions. The dominant color is red, but the limestone ledges are gray. Salt Valley anticline's northeast flank contains a great exposure of the basal sandstone of the Tidwell Member (fig. 22). The Tidwell Member is approximately two feet thick and a yellow-gold in color. The ripple marks found in the basal sandstone indicate a flood plain deposition in quiet shallow waters.

There appear to be no regional trends or any response to local salt movements within the Tidwell Member because the thickness in the Salt Valley Anticline area averages approximately 65 feet throughout (Doelling, 1988). Thickness determined by a three-point calculation for a site in Township 22S and Range 20E is 45 feet. This measured thickness differs from Doelling's (1988) average thickness because within the study area, the Tidwell Member is exposed and has been subjected to erosion. The location of the three-point calculation was evidently in an area where approximately 20 feet of the Tidwell Member had been eroded away.

Salt Wash Member. Conformably overlying and interfingering with theTidwell Member is the Salt Wash Member. The lithology of the Salt Wash Member is more inhomogeneous than the other units in the area. It consists of several types of lithologies, such as fine-to-coarse-grained sandstones, conglomerates, quartzite, mudstone, siltstone, shale, and limestone that make up rough, chunky, loose, and rocky outcrops with several boulder-sized float pieces (fig. 23; Doelling, 1988). Interstratified sandstone and siltstone make up the dominant lithology (Craig and Cadigan, 1958).

The Salt Wash Member forms benches and dip-slopes, and weathers to earthy slopes (Doelling, 1988). Cross-laminated beds show an irregular basal scour surface (fig. 24; Craig and Cadigan, 1958). The color of the Salt Wash Member varies from light gray to yellow, green, and pale orange. The depositional environment appears to be fluvial, with sandstone chunks representing individual river channels (fig. 25). The Salt Wash

Figure 23. Saltwash Member of the Morrison Formation appears as a very rocky outcrop with much boulder-size float.

Figure 24. Sand channel of the Salt Wash Member of the Morrison Formation showing boulder with cross-laminated beds. The top, flat slab of the Moab Tongue is seen in the background.

Figure 25. Traceable old meandering river channels represented by the Saltwash Member of the Morrison Formation. Traces of river channels are are indicated by white lines.

Member displays several stratigraphic features: meanders, bars, trough cross stratifications, cut and fill, and overbank deposits (Doelling, 1988). Petrified and carbonized wood fragments are found throughout and are a result of trees that were uprooted along the streams as meandering and flooding took place during deposition (Doelling, 1985). The Salt Wash Member is well known for its dinosaur bones, but the sandstones also contain uranium, copper, and vanadium minerals in certain areas.

The regional thickness of the Salt Wash Member ranges from 132 to 300 feet (Doelling, 1988) and is determined by solving a three point problem for a site in Township 22S and Range 20E to be 180 feet in the study area.

Brushy Basin Member. The Brushy Basin Member comprises the top of the Morrison Formation (fig. 26). It interfingers with the underlying Salt Wash Member. Sandstone and conglomerates are well developed near the bottom of the unit, resembling those of the Salt Wash Member. The maroon to pale green color of this unit reflects the muddy siltstones, sandstones, limestones, and swelling clays found within it. The swelling clays are derived simply from the hydrolysis and devitrification of volcanic ash. The Brushy Basin Member forms steep outcrops with smooth slopes.

There are a two different depositional environments that existed during the deposition of the Brushy Basin Member. The muddy siltstones came from a flood plain depositional environment. They were a result of major rivers flooding and producing overbank deposits. The limestone and shale are characteristic of an interfluve environment.

The regional thickness is 300 to 450 feet. A three-point calculation for a site in Township 22S and Range 20E yields a thickness of 325 feet. The thickness is relatively

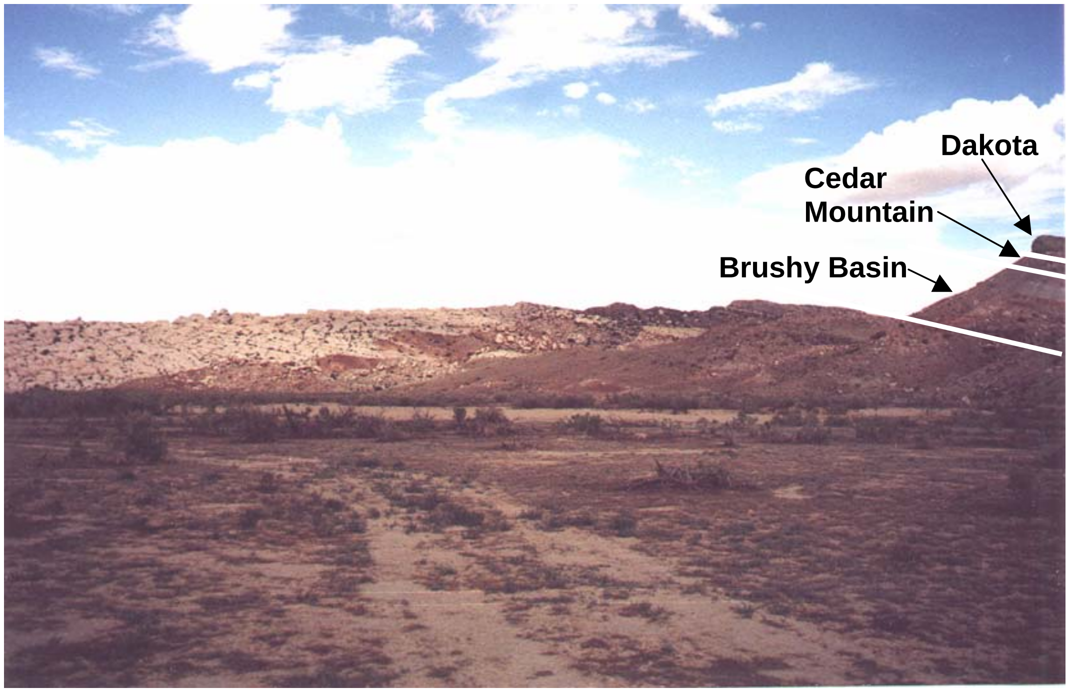

Figure 26. Brushy Basin Member of the Morrison Formation, and Dakota and Cedar Mountain Formations.

uniform across the anticline, suggesting that the salt was not actively flowing during deposition (Doelling, 1988).

Cretaceous Stratigraphy

Cedar Mountain Formation

The Cedar Mountain Formation conformably overlies the Morrison Formation and is separated into two units: the lowermost sandstone, conglomerate and limestone, and the silty or shaly mudstone upper unit (fig. 26). Chert, petrified wood, and some fossils are found within the Cedar Mountain Formation (Doelling, 1988). The lower portion forms ledgy outcrops (Molenaar, 1981). In the study area, only the lower cliff-forming unit is present because the overlying silty mudstone above it has been eroded (Doelling, 1988). The overall hue of the Cedar Mountain Formation is dark brown to black. The Cedar

Mountain Formation developed in a flood plain and fluvial depositional environment (Molenaar, 1981).

The regional thickness of the entire Cedar Mountain Formation is 100 to 250 feet (Doelling, 1988). However, the thickness in the study area of the lower unit is approximately 15 feet by visual observation in Township 22S and Range 20E. The thickness of the Cedar Mountain Formation was measured on the upper portion of the west flank of Salt Valley Anticline. In general, the formations thin over the top of the anticline. Thus, the Cedar Mountain Formation is thinner at the top of the flank than at the bottom.

Dakota Sandstone Formation

Disconformably overlying the Cedar Mountain Formation is the Dakota Sandstone. This dark brown to black unit consists of conglomeratic channel sandstone, shale, and coal (Molenaar, 1981). The formation forms hard sandstone ledges with black chert (Doelling, 1988). In certain places, marine sandstone tops the formation (Molenaar, 1981). The presence of *Halymenites* indicates a marine depositional environment for the unit; however, the conglomerates and sandstones, along with fossil wood and leaves, are indicative of a fluvial depositional environment (Doelling, 1988). Doelling (1988) suggested that the marine and continental units inter-tongue. The Dakota Sandstone was deposited on a broad coastal plane that was later inundated by the advancing Mancos Sea. Occasional plant fossils are the only way to identify its Late Cretaceous age.

The thickness of the Dakota Sandstone Formation is rather uniform over the area. Regionally, the thickness only ranges from 20 to 80 feet. By a three-point calculation for a site in Township 22S and Range 20E, a thickness of 20 feet was obtained. Salt movement is not responsible for any apparent change of thickness since the thicknesses of the Dakota Sandstone within the crest of Salt Valley Anticline vary to the same degree as at other locations in the region. The Dakota Sandstone is at its minimum thickness over the anticline crest. This is due to the fact that it is exposed and subjected to erosion since the overlying Mancos Shale has been eroded completely. Most of the formation is exposed as cobble conglomerate due to the salt dissolution collapse of Salt Valley Anticline (Doelling, 1988).

CHAPTER FOUR

Structural Geology

Overview

The structural geology of the Salt Valley Anticline crest is highly complex. It is erosionally breached by Salt Valley, with the east side structurally higher than the west (fig. 27; Dane, 1935). Normal faults bound each side of the valley, dropping the valley floor far below the crest of the anticline (Kitcho, 1981; Dane, 1935). The valley is a graben structure approximately one-half mile in width with a trend of N43W. Resistance to erosion has left the flanks of Salt Valley Anticline standing as ridges that are inclined gently to moderately away from the crest of the anticline within a range of five to twenty-five degrees (fig. 21). The study area is located on the more structurally complex, west flank of Salt Valley Anticline. The two dominant brittle structures found in the study area are joints and faults.

Joints

Description

The Colorado Plateau has a regional joint pattern that passes through the study area and entire stratigraphic section (Suppe, 1985). These regional joint sets generally trend northeast and northwest (Woodward-Clyde Consultants, 1983). In the study area, joints are most pronounced on the limbs, as contrasted with the hinge zone, of Salt Valley

A.

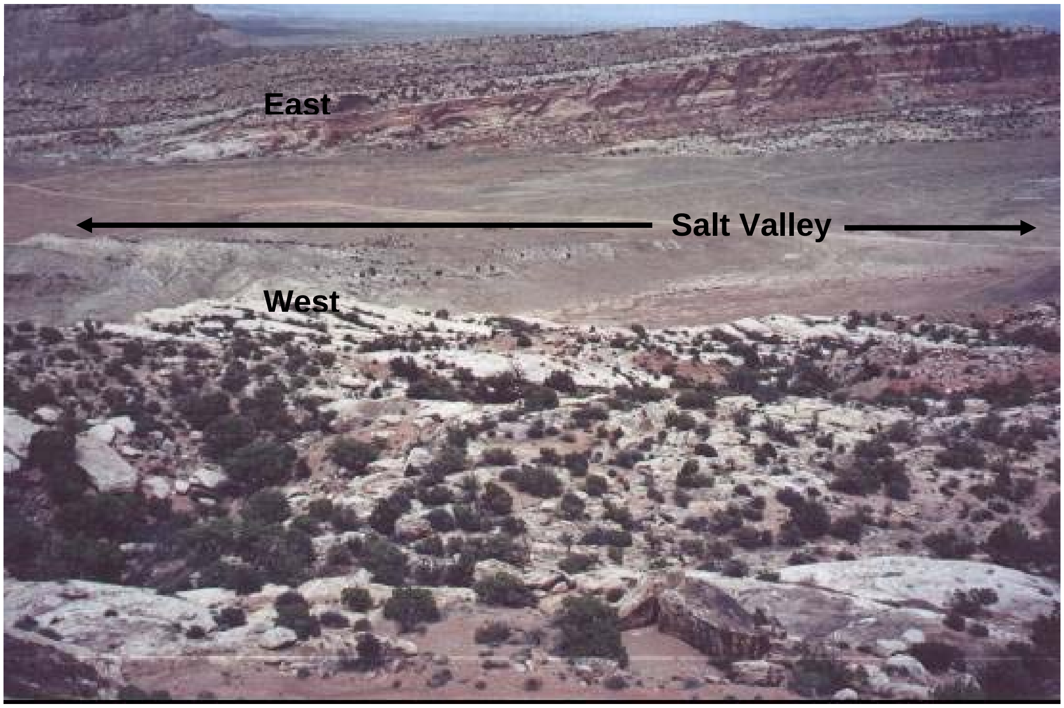

B.

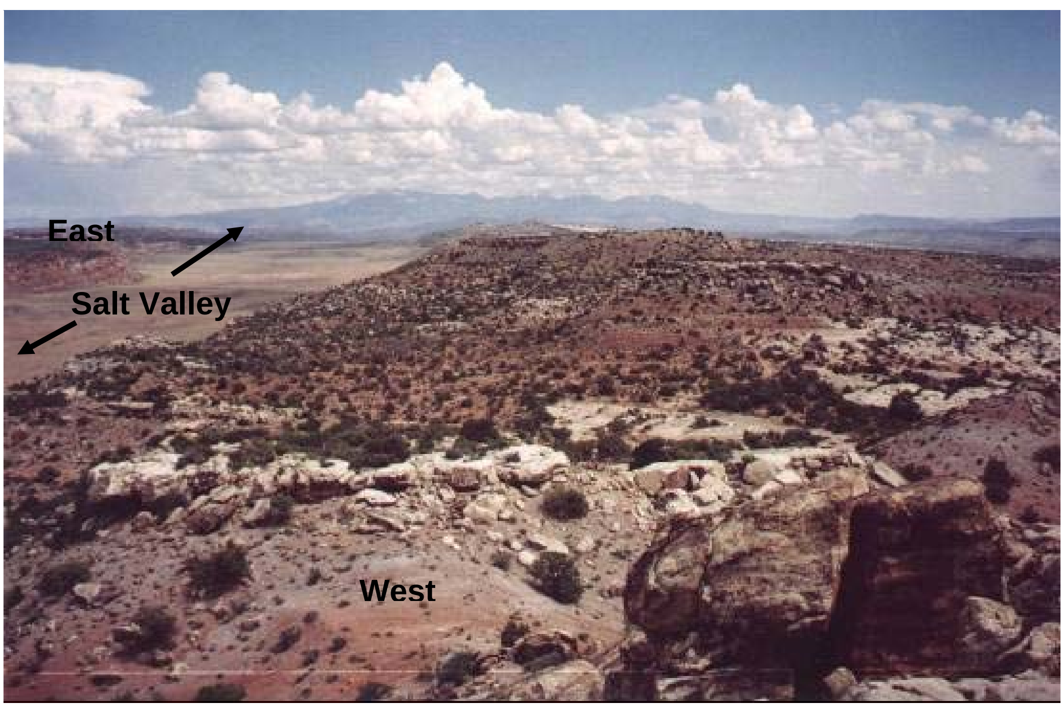

Figure 27. (A) Crest of Salt Valley anticline in northern part of the study area, looking northeast. (B) Crest of the anticline in the southern part of the study area looking southeast. Salt Valley is bordered by steep normal faults that have dropped the valley below the crest of the anticline.

Anticline. Joints exposed at the ground surface in the study area are only found in the brittle Moab Tongue Member and are most apparent as observed in aerial photographs (plate 1). Joints appear as continuous lineaments on aerial photographs, but are commonly more discontinuous when observed on the ground (fig. 14; Trudgill and Cartwright, 1994). In some cases, apparently continuous joints observed on aerial photographs are actually several sets of joints arranged *en echelon* as observed on the ground.

The study area contains one joint system with three sets of joints, each set with its own distinctive orientation, spacing, and length (fig. 28). These sets include joints that are parallel, perpendicular, and oblique to the hinge of the Salt Valley Anticline (fig. 29). In all three sets, the joints are symmetric, sub-parallel, and evenly spaced. However, there is an area on the crest of Salt Valley Anticline that is considered nonsystematic with short, irregular joints that are not part of a specific joint set (fig. 30).

Set One

Joint set one is classified as oblique joints because it forms a 45 degree angle with the axis of Salt Valley Anticline. The strike orientation of the joints is ~N26W, ranging from N34W to N1W (fig. 31). The average length of the joints in this set is 364 feet, with a prominent joint spanning 1,965 feet (fig. 32). The smallest joint measured in the set was 20 feet long. The lengths of the joints in set one seem to be generally longer than in the other sets.

The location of joint set one is primarily in the center of the study area. No joints in this set are found on the perimeters of the study area. The most prominent joint is located at the southernmost edge of the set. Within this group of joints, it is unclear if joint set one curves northwest into a different orientation or merges with another joint set.

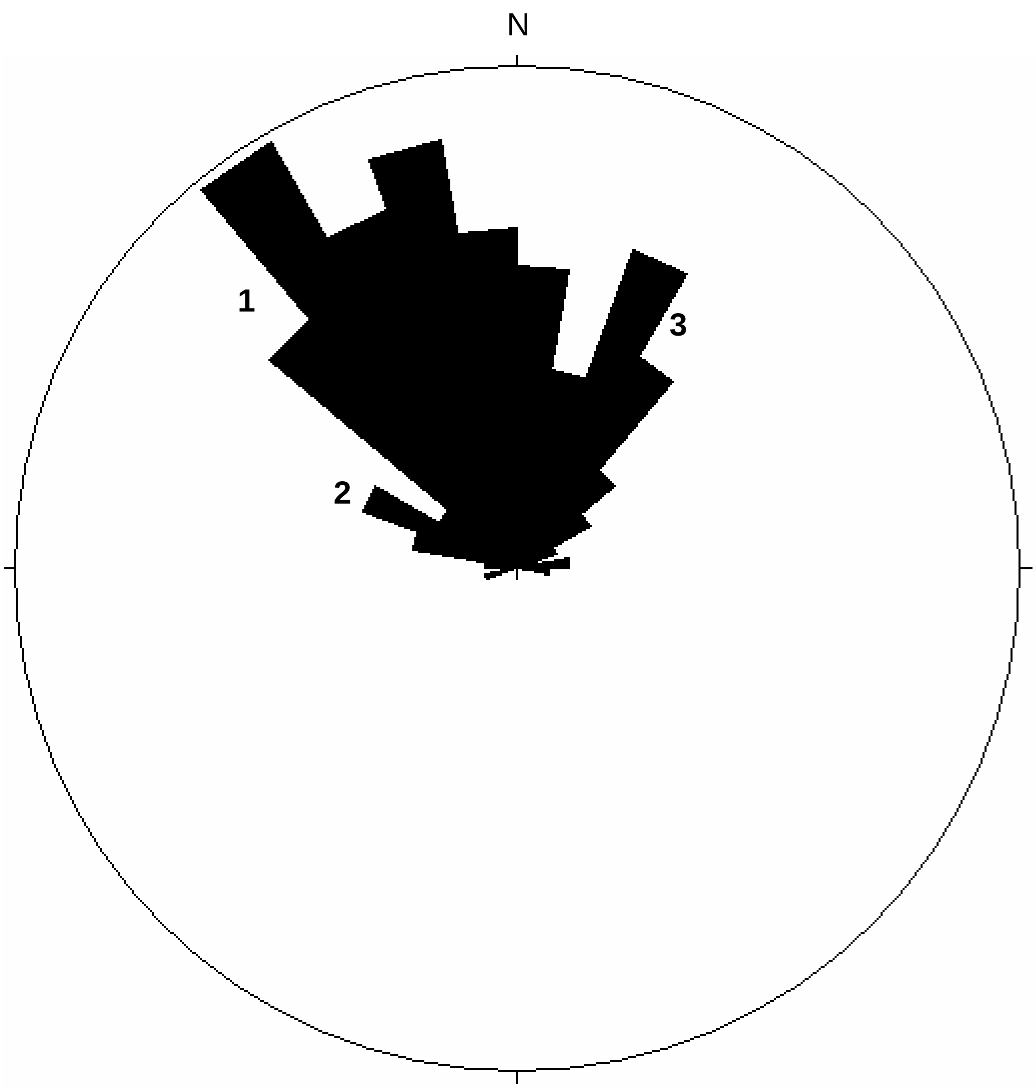

Figure 28. Rose diagram of strikes of joints in study area with the three sets labeled.

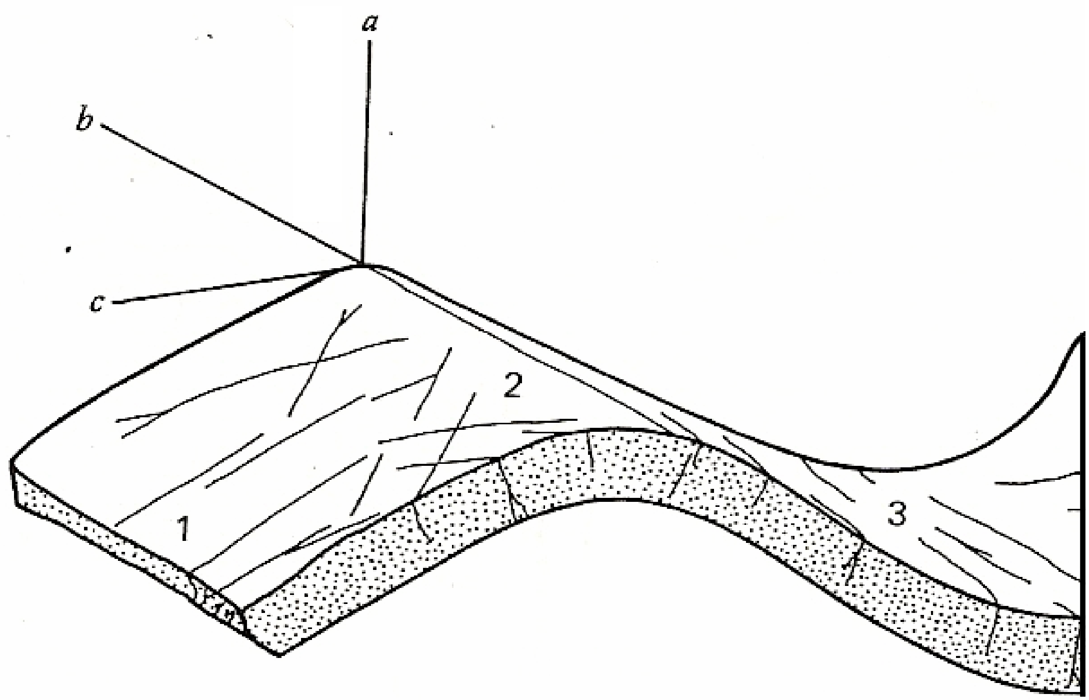

Figure 29. The three categories of joints found in the study area, (1) cross joints, (2) oblique joints, and (3) longitudinal joints as they appear in relation to folded rocks. Modified from Hobbs and others (1976).

Set Two

The most prominent joint set in the study area is set two. Joint set 2 spans the entire length of the study area and contains 604 measured joints -- three times more joints than the other two sets. The average length of joints in set 2 is 238 feet, with a maximum length of 1,445 feet. No particularly prominent joints were observed in set 2. This may be due in part to sediments covering the majority of the length of the joints.

Joint set two is approximately parallel to the strike of the axial plane. The average strike is N69W, ranging from N89W to N56W. The joints of this set parallel one another more closely than the other two sets are is located closest to the faults of the Salt Valley Anticline hinge zone.

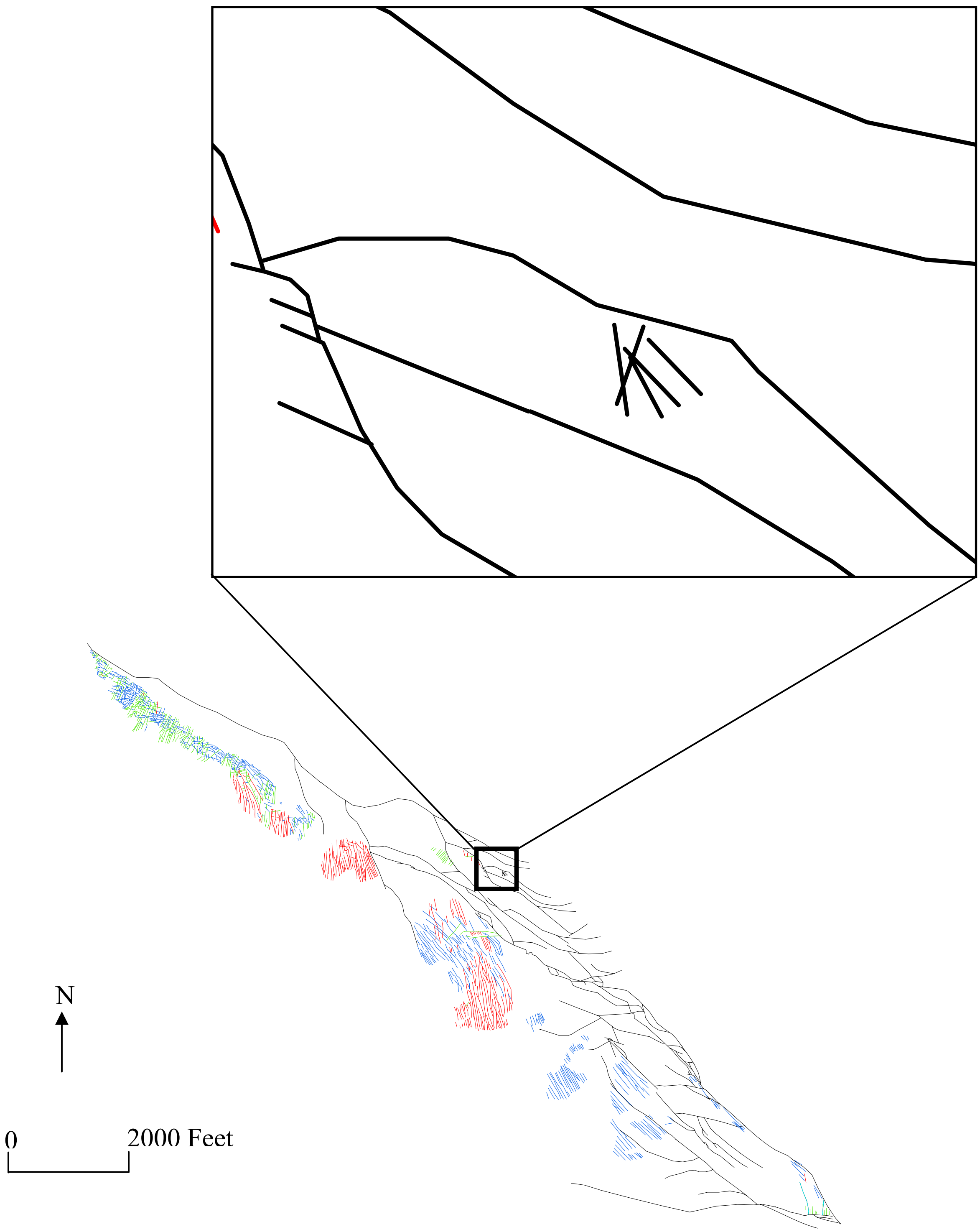

Figure 30. Nonsystemic, short, irregular joints that are not part of a joint system are found between two faults and are indicated with an arrow.

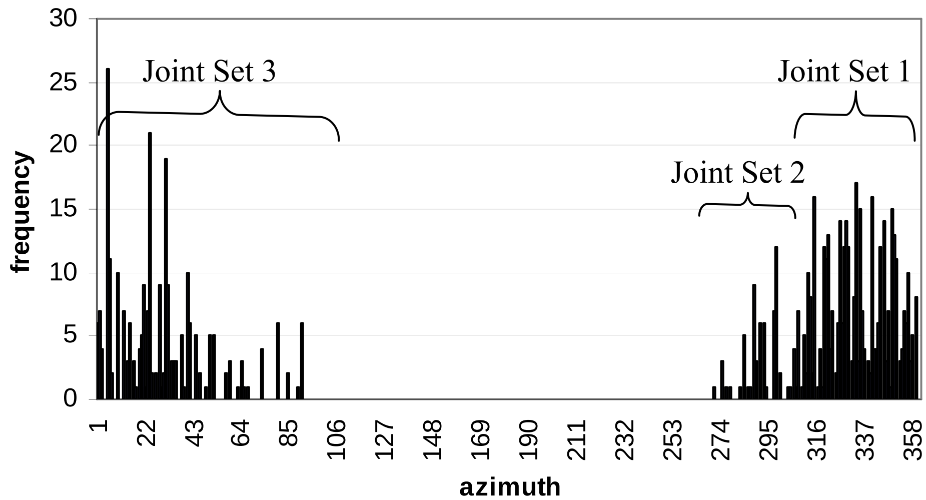

Figure 31. Histogram of all three joint sets showing strong northwest and northeast orientations.

Set Three

The third set is located at either end of the study area and contains 260 measured joints with an average length of 216 feet. The minimum length is less than one foot and the maximum is 1,393 feet. The majority of joints are very short. The joints in set three are more closely spaced than the joints in the other two sets. The average strike of set three is N28E, with a range of N0E to N90E.

Faults

Description

The faults observed along the crest of Salt Valley Anticline are essentially all normal faults. A total of 90 normal faults oriented sub-parallel to the anticline axis were mapped and measured. These faults can be subdivided into two fault systems (A and B) based on

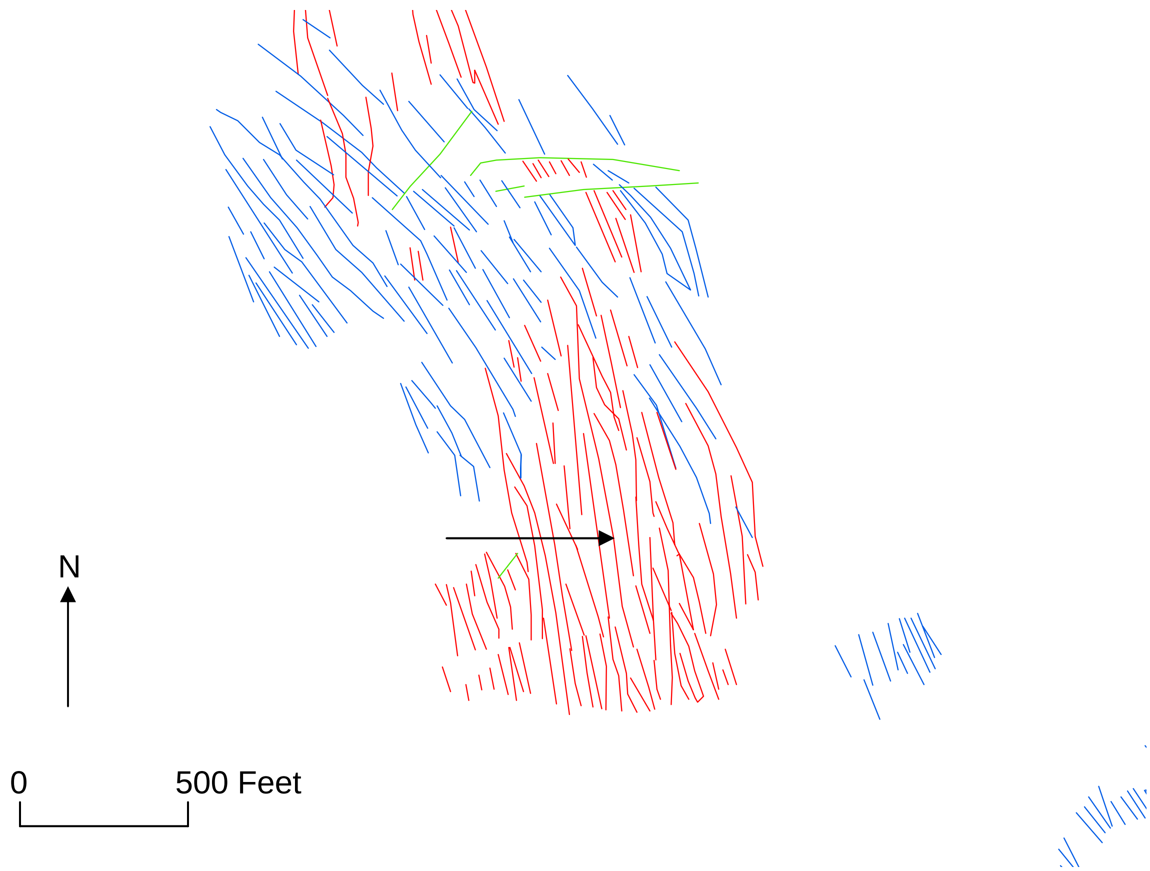

Figure 32. Joint set one (red) has an average individual joint length of 364 feet and a prominent joint with a length of 1,965 feet, located in the middle of the study area and indicated with arrow.

fault orientation and arrangement (fig. 33). Both systems span the length of the study area. Most of the faults in the study area dip at moderate to steep angles, averaging 64 degrees. Approximately 95 percent of the faults dip steeper than 45 degrees, but no vertical faults were mapped in the study area.

Several horst and graben structures are present in the study area (fig 34). Cross section A-A’ contains two grabens (fig. 7). The grabens, although down-dropped, are located at the two maximum elevations of the cross-section.

There are also a number of relay ramps in the study area (fig. 35). Relay ramps are structures created when two synthetic, normal faults grow past one another and transfer displacement. The “ramp” is rotated to reflect the displacement transfer. Since relay ramps form through the amalgamation of shorter faults to form one long, through-going fault, there are different developmental, or evolutionary, stages (fig. 36). There is an underlap stage, where the faults have little or no interaction, an overlap stage where fault interaction is heightened, and a breach stage where the two faults are joined. In the breach stage, the faults may join by curving, or hooking, into one another, or a cross-trending fault may form and connect the two faults.

Shear displacement along a fault surface under low pressure-temperature conditions characteristic of near-surface deformation generally produces thin scratches (striae) or thicker grooves that are collectively known as slickenlines (fig. 37). The direction of the most recent shear displacement along the fault is parallel to the slickenlines. Approximately 23% of fault surfaces observed in the study area contained slickenlines

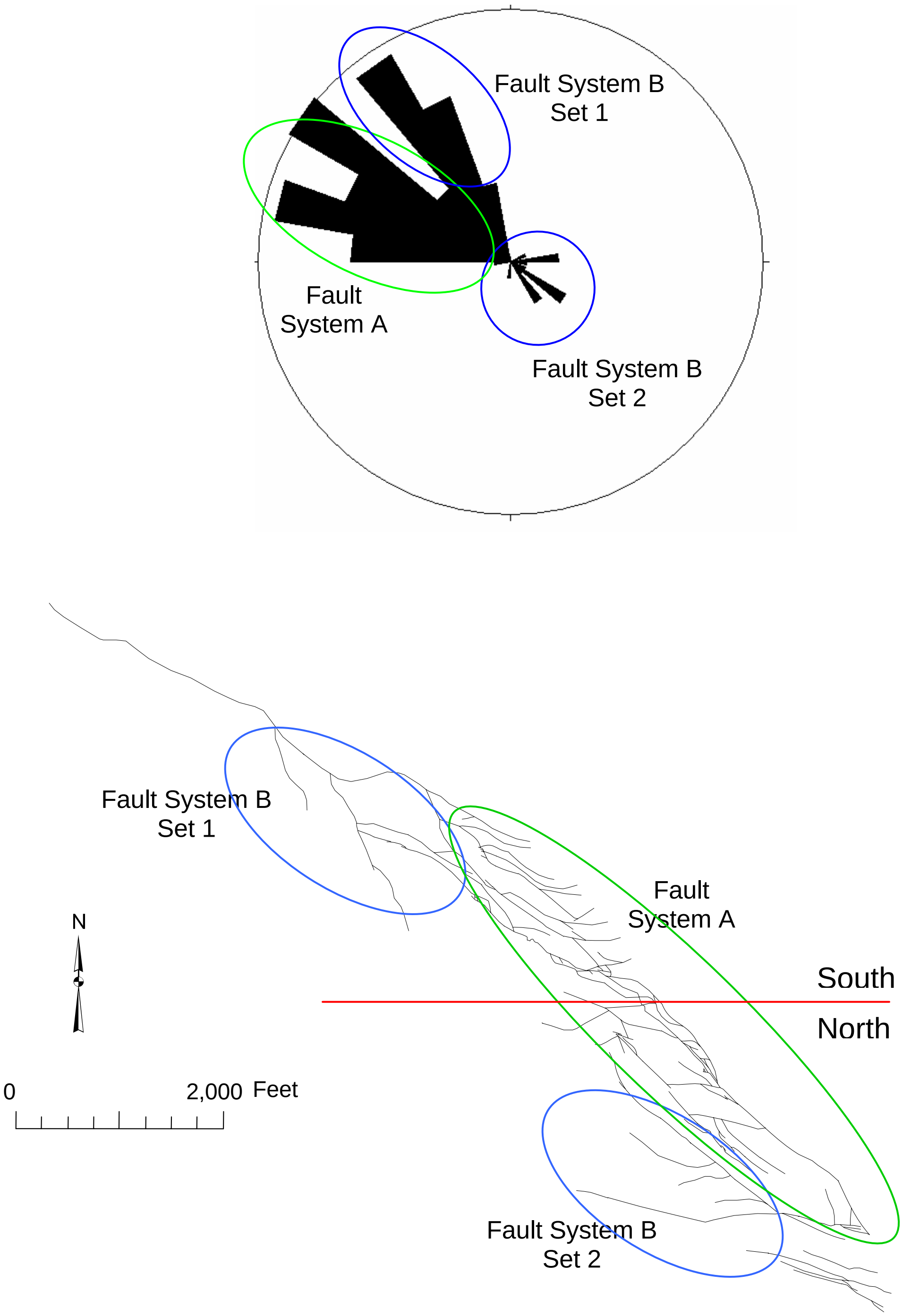

Figure 33. The area is subdivided into two fault systems, A and B, based on fault orientation and arrangement. (A.) Rose diagram for both fault systems. Fault system A is circled in green and fault system B is circled in blue and labeled for the different fault sets. (B.) Map view of fault systems, circled in green (fault system A) and blue (fault system B), with a red line dividing the north and south regions for description purposes.

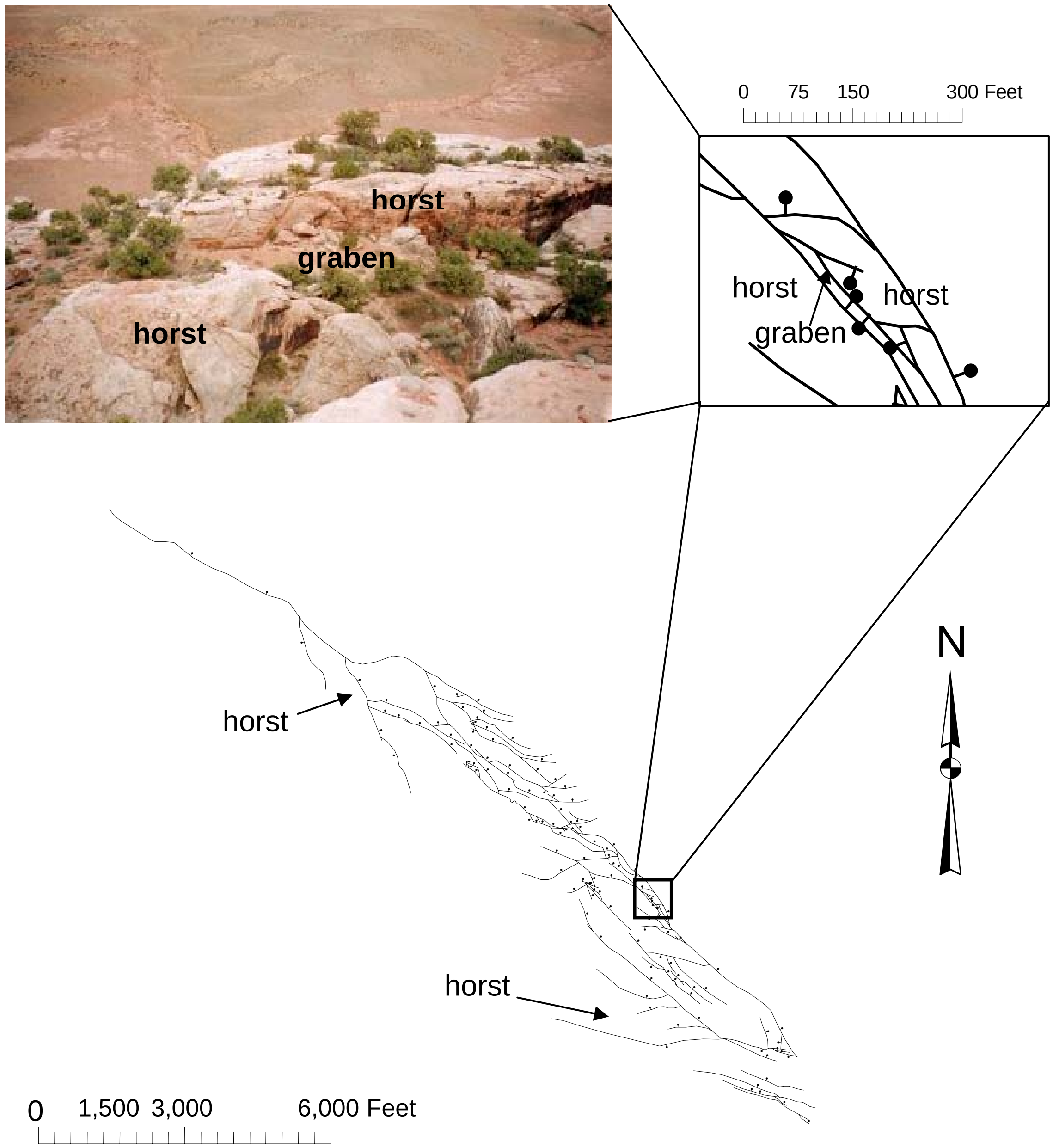

Figure 34. Location maps and field photograph showing horst and graben resulting from movement on antithetic faults. View of photograph is to the east.

A.

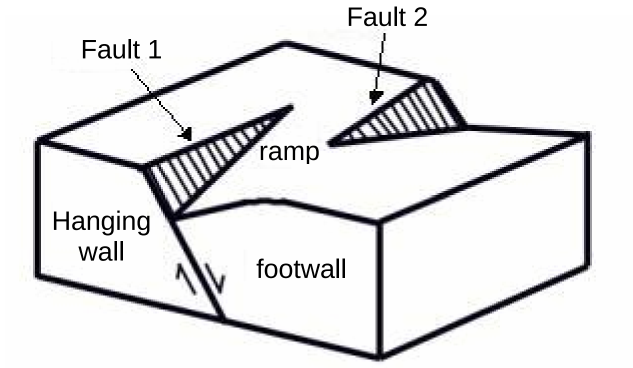

B.

Figure 35. (A.) Block diagram of a relay ramp between two normal faults with the same sense of throw. The ramp connects the hanging wall and the footwall. Modified from Larsen (1988). (B.) Photograph of breached relay ramp showing two normal faults growing past each other and one terminating against the other. Photograph taken in the northern region of the study area, view to the southeast.

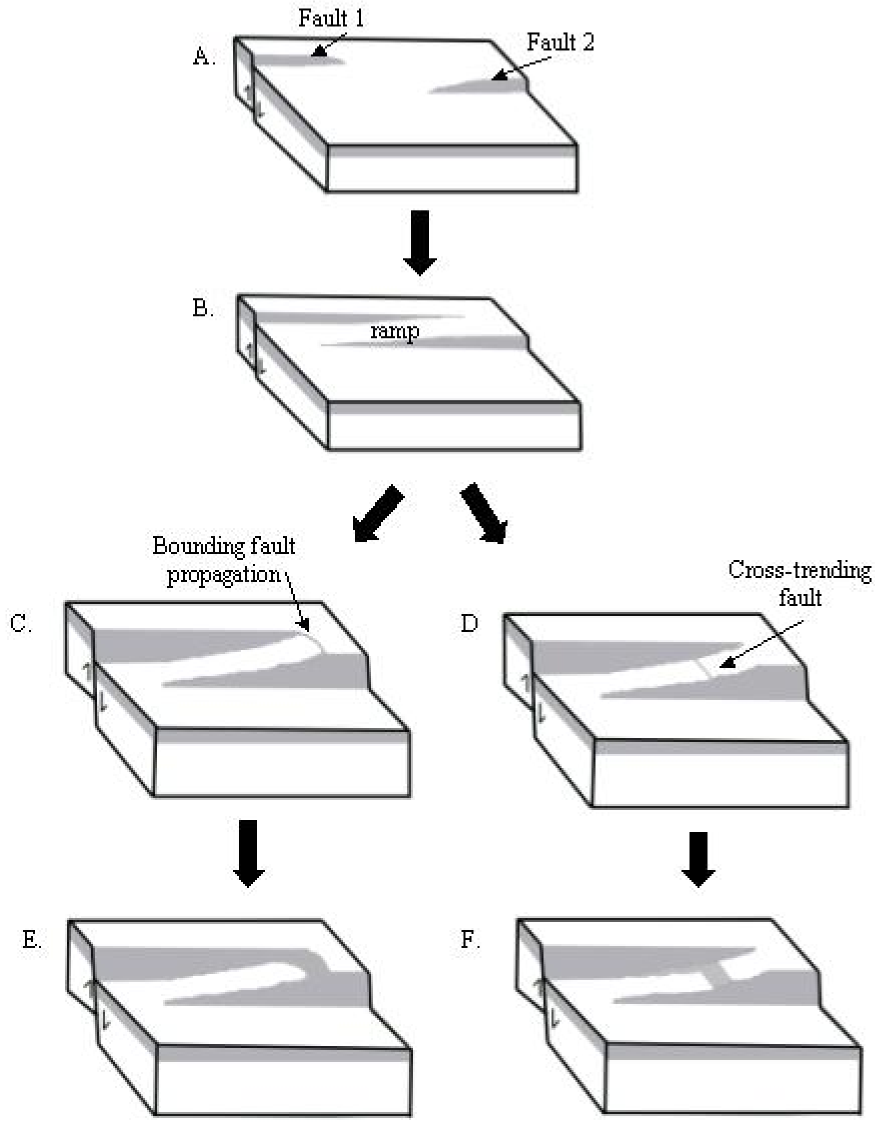

Figure 36. Evolution of a relay ramp.. (A) Under-lap stage: two normal faults with the same sense of throw propagating past one another. (B) Over-lap stage: the formation of a relay ramp connecting the hanging wall and footwall. (C, D) Early-breach stage: The breaching of the ramp by the propagation of one of the bounding faults or a cross-trending fault. (E, F) Late-breach stage: the complete separation of the hanging wall and footwall. Modified from Peacock and Sanderson (1994)

Figure 37. Photograph of fault surface showing slickenlines. Photograph taken in the middle of the study region with a field of view approximately three feet.

Fault System A

Fault system A is a parallel relay array with the faults paralleling each other and transferring displacement via relay ramps. Fault system A is located on the crest of Salt Valley Anticline and the orientation of the faults roughly parallels the Salt Valley Anticline axis, trending northwest to southeast. Fault strikes range from N32W to N88W and average N62W, with an average dip of 64 degrees.

Fault system A includes 78 percent of the faults in the study area. A stereonet plot of the poles to the planes of the faults illustrates that the faults are tightly clustered (fig. 38). Average spacing between individual fault segments is 250 feet and the average length of a fault in this system is 1960 feet. Nineteen relay ramps are found within fault system A. Cumulative displacement across the relay system is relatively constant. Fault scarps are more prevalent in fault system A than in fault system B. Very distinct, smooth surfaces were present on the majority of the faults.

Fault System B

Fault system B is located on the west flank of Salt Valley Anticline. It is a conjugate array containing two fault sets with a dihedral angle of approximately 65 degrees. Each fault set of this system tends to curve in towards the local fold axis. Antithetic normal faults of both fault sets have created horsts whose trends make an angle of approximately 40 degrees with the anticline axis (fig. 34).

Set One. Fault set one is located in the north region of the area and is orientated northwest to southeast. The faults parallel and strike within 23 degrees of each other. The average

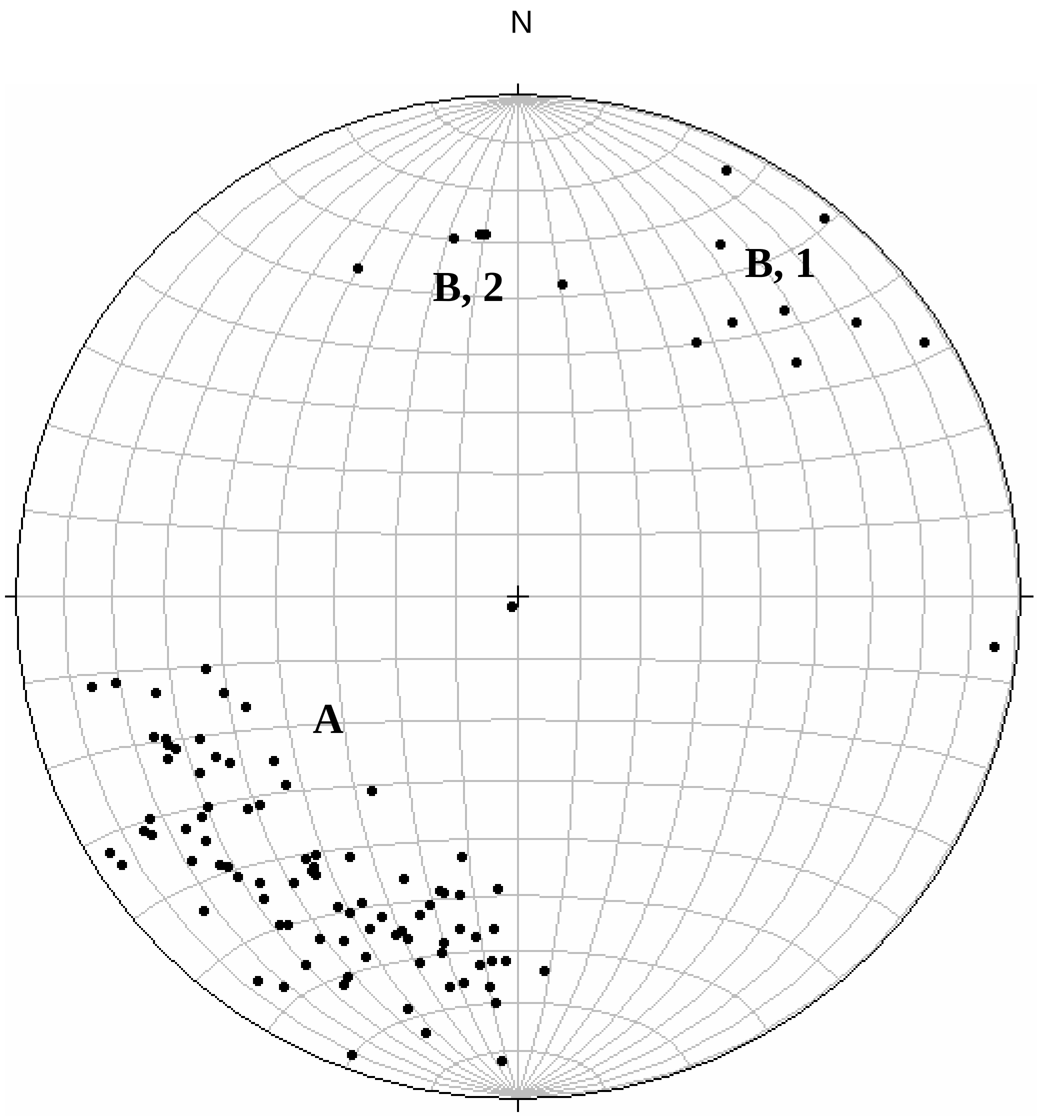

Figure 38. Schmidt equal-area stereonet plot with lower-hemisphere projection of the orientation of the poles to the fault planes in the study area. Fault systems are annotated.

strike and dip is N22W and 63 degrees. Set one is comprised of only 10 fault segments with an average length of 1,342 feet. Spacing between each fault is approximately 824 feet.

Set Two. Fault set two is located in the south region and is oriented northeast to southwest. Much like fault set one, fault set two is comprised of paralleling faults that strike within two degrees of each other. The average strike and dip is N95E and 66 degrees. Spacing between the faults of set two is noticeably smaller than set one at 595 feet.

CHAPTER FIVE

Discussion and Conclusions

Overview

The joints and faults of the study area provide physical evidence that helps us to unravel the story of the Salt Valley Anticline. Two major structural events occurred: the formation of the Salt Valley Anticline and its subsequent collapse. I infer that these structures are related to regional extension across the area.

Anticline Formation

Regional extension and consequent salt movement are interpreted to be the underlying causes of the formation of Salt Valley Anticline. Extension caused normal faulting to develop in the section above (and perhaps below) the salt horizon. Salt moved laterally toward areas where extensional thinning of the overburden had lessened the pressure. The salt was concentrated and rose into the faulted section. As the salt rose forming a wall, the overburden arched into an anticline (fig. 39). The extension rate was

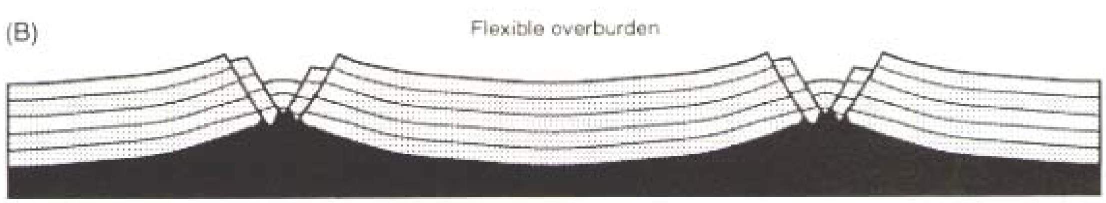

Figure 39. Flexible overburden being arched into an anticline over rising diaper. From Vendeville and Jackson (1992a).

fast enough so that the salt was able to pierce the overburden, but not so fast that the salt would be trapped below numerous normal faults (fig. 40; Vendeville and Jackson, 1992a).

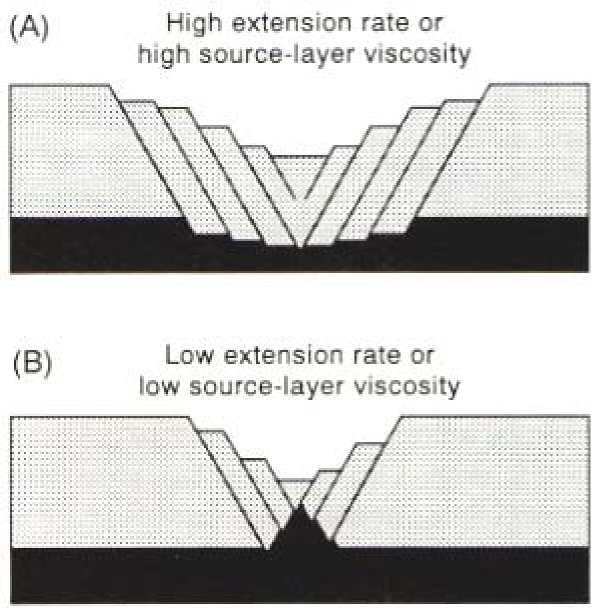

Figure 40. Comparison between graben formation and diapir rise with a high extension rate (A) and a low extension rate (B). From Vendeville and Jackson (1992a).

Joints typically form as a result of extension. In homogeneous, isotropic material, mode I extension cracks form parallel to the greatest principal compressive stress (σ_1) and perpendicular to the least principle compressive stress (σ_3). Hence, they form with no shear stress on their faces, and the displacement is directed normal to the joint surfaces (*e.g.,* Hobbs and others, 1976). Vertically-oriented, regional joint sets that extend over hundreds of miles seem to develop parallel to the direction of greatest horizontal stress (S_H) and perpendicular to the least horizontal stress (S_h) at the time the joints form (*e.g.,* Engelder, 1993).

Experimental models suggest that regional extension can significantly affect fault patterns on salt domes (fig. 41; Withjack and Scheiner, 1982). On salt anticlines without extension, Withjack and Scheiner (1982) found that normal faults rarely develop on the flanks of the anticlines and are localized on the crest. Salt Valley Anticline underwent extension and has few if any faults, only joints, on the flanks. Faults occur primarily along the crest.

The spatial relationship of different joint sets can be studied in hope of determining the relative ages of joints. Younger joints terminate against older joints. Younger joints can hook and terminate perpendicular into the older joint (Wheeler and Holland, 1978).

The joints of joint sets two and three crosscut one another without apparent deflection (fig. 42). These two sets formed first in the evolution of Salt Valley Anticline. The observation that mode I joints sometimes cross one another without displacing one another leads to an interesting problem. In the past, the similarity in the conjugate geometry of some cross-cutting joints to the conjugate geometry of faults developed in laboratory deformation experiments suggested to some that the maximum principle stress axis could be assumed to bisect the acute dihedral angle, and the minimum principle stress bisected the obtuse angle. The fallacy in this reasoning is that experiments produce conjugate faults (mode II shear cracks) in one deformation episode and not conjugate joints (mode I extension cracks). An alternative explanation is that the conjugate joint geometry observed in the field is the result of a series of different stress states over an

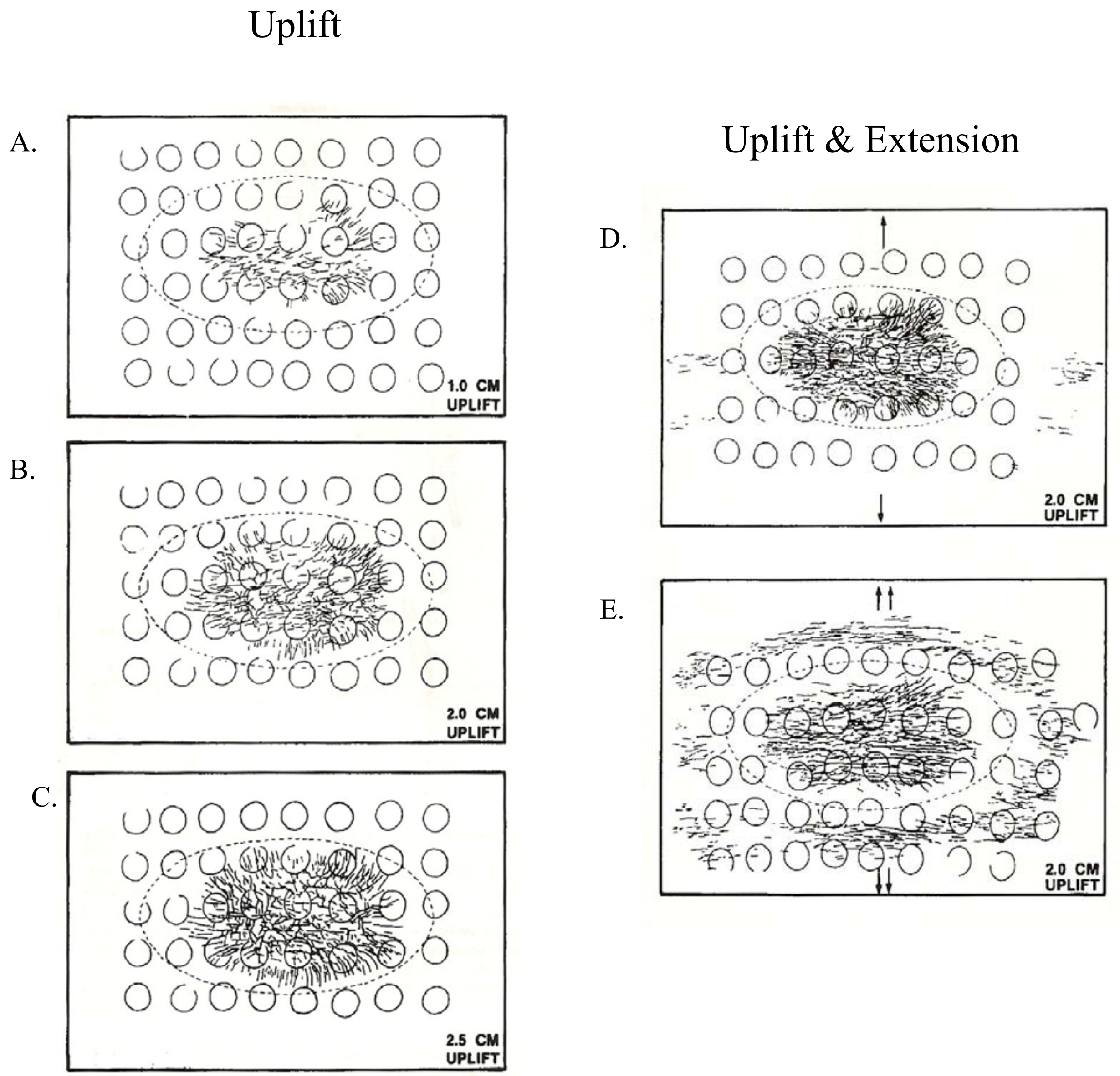

Figure 41. Clay model experiment with (A.) faults forming parallel to the long axis of the dome at 1 cm. of uplift, (B.) faults forming perpendicular to the axis at 2 cm. of uplit, and (C.) faults lengthening and reaching the periphery of the dome at 2.5 cm. of uplift, and (D & E.) uplift with applied extension at 2 and 2.5 centimeters of uplift and faults forming parallel to the long axis of the dome on the crest and flanks. From Withjack and Scheiner (1982)

Figure 42. Intersections of faults at approximately right angles. The faults mutually cross-cut one another with no disturbance.

extended period of structural evolution rather than a single stress state and concurrent jointing (fig. 43).

Imagine a tabular formation that is mechanically homogeneous and isotropic at some initial time t_0 (fig. 43A). At a subsequent time t_1, the layer is subjected to a layer-parallel differential stress sufficient to result in mode I extensional failure in the σ_1-σ_2 plane (fig. 43B). At time t_2, a differential stress is applied to the layer in a different direction (fig. 43C). The component of stress acting normal to the open joints results in closure of the joints formed at t_1 so that the two joint faces are in contact with one another. With the original joints closed, a new joint system develops parallel in the new σ_1-σ_2 plane, cross-cutting the original joint surfaces. Finally, the layer is exhumed by erosion, and all of the joints open as the lithostatic pressure associated with the eroded overburden is removed (fig. 43D).

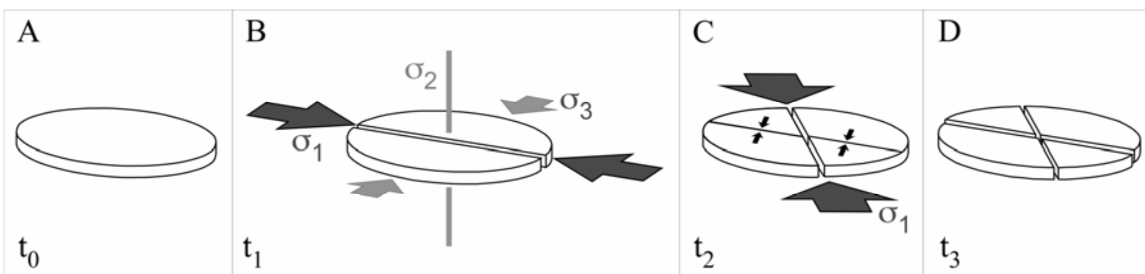

Figure 43. A conceptual model for the development of conjugate joints. (A) Initial state at time t_0. (B) Mode I extensional joint develops in σ_1-σ_2 plane. (C) In a different stress field, the initial joint is closed and a new joint develops in the σ_1- σ_2 plane. (D) Both joints open during erosional exhumation. Figure by Cronin for this thesis.

It is not established whether joint set two or three developed first, because the joint faces were not examined to investigate possible nucleation points or deflection of plume marks that would indicate the relative timing of joint formation. Joint set one, which formed last, appears to exhibit en echelon segments.

The primary joints observed in the field area are oriented subparallel to the hinge surface of the anticline. There are two related processes that may be reflected in the developmental history of the joint sets: regional extension and local salt diapirism. The NE-SW regional extension would generally favor development of NW-SE striking extensional joints and normal faults. Motion on NW-SE striking normal faults in the subsalt basement would localize the development of salt walls (elongate salt diapirs) striking parallel to the normal faults. Horizontal folding of a brittle upper layer would be expected to result in extensional or even tensional failure along the upper surface of the layer, with mode I extension cracks developing strike-parallel to the hinge with crack faces approximately perpendicular to the layer's folded surface. Both the regional extension and the salt diapirism would be expected to result in mode I extensional joints striking NW-SE.

A gradual variation in strike is observed from the northern part of the study area to the south. This change in joint orientation occurs coincident with the change in orientation of the Salt Valley Anticline fold axis, strongly indicating that the joints are related to stresses imparted to the jointed formations during or after folding.

The presence of joints may enhance the overall permeability of a rock volume, affecting groundwater as well as hydrocarbons. Studying the characteristics and development of joints may allow petroleum geologists to make an estimate of formation reservoir quality. Fluid flow along joints may also lead to the precipitation of mineral deposits (Davis and Reynolds, 1996). Where jointed rock exists in highland areas above roadways or other engineered works, they may contribute to landslide or rockfall hazards.

Anticline Collapse

The majority of joints were formed during anticline formation, but some may have formed during the anticline collapse (Doelling, 2000). As Salt Valley deepened and widened, the crest of Salt Valley Anticline collapsed into the valley. Joints formed in the brittle sandstone as it was flexed (fig. 44). With continued anticline collapse, shear displacement may have turned some favorably oriented joints into faults.

Whether or not a relay ramp will breach depends primarily on the displacement of the bounding faults (Ferrill and Morris, 2001). Within a breached relay ramp, the linkage point is marked by a decrease in total displacement (Peacock and Sanderson, 1990). This decrease in displacement is cause by the fault that breaks the ramp (Peacock and Sanderson, 1991) and may be reflected in the rotation of the relay ramp (Peacock and Sanderson, 1990).

Relay ramps have important hydrocarbon implications. Unbreached ramps may be migration paths for fluids to and from both the hanging wall and footwall (Larsen, 1988). These ramps may allow hydrocarbons to escape from a reservoir or basin, with oil flowing up the ramp (Peacock and Sanderson, 1994). Breached ramps, however, may trap hydrocarbons. The breach, or fault, may provide strike closure or a fault seal (Peacock and Sanderson, 1994). These breaks may also provide paths of communication between aquifers and oil reservoirs which otherwise would be compartmentalized (Kattenhorn and Pollard, 2001). The extension of relay ramps, accommodated by

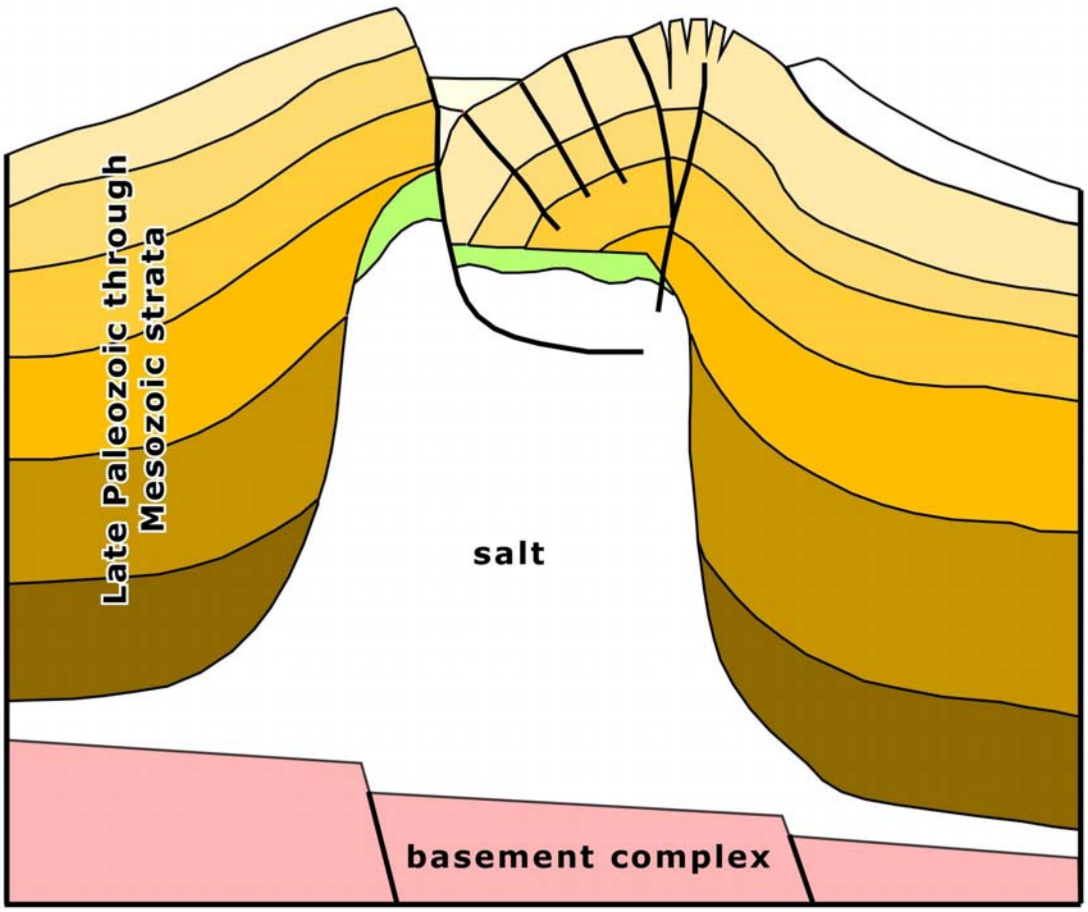

Figure 44. Joints formed on the crest of Salt Valley Anticline due to rollover. From Doelling (2000).

faulting and fracturing, increases the porosity and permeability throughout oil and water reservoirs (Ferrill and Morris, 2001). By recognizing these breaks, petroleum geologists can gain information about the sealing effectiveness of the reservoir (Kattenhorn and Pollard, 2001). Relay ramps may also exert and effect on the local topography, outcrop patterns, stratigraphy, erosion and drainage (Peacock and Parfitt, 2002).

Suggestions for Further Work

As with any study, the scope of this thesis research was constrained by a number of limiting factors. Consequently, this work constitutes a useful starting point for a number of potential future studies.

Current availability of surveying-grade GPS and laser-rangefinding technologies present the opportunity to map the ground surface as well as the locations of joints and faults with unprecedented accuracy and resolution. It is possible that data from an aerial LIDAR (light detection and ranging) survey can be obtained for the area, which is quite suitable for this application because of its relative aridity and lack of vegetative cover. Better topographic data would enable the development of a digital elevation model for the area that would be useful in geologic mapping (Maune, 2001). The ability to manage these data in a geographic information system (GIS) permits us to merge, analyze and produce georeferenced maps of many different types of data. This research project has provided a hint of the potential of these technologies for field geologic studies, which can be amplified in future work.

It would be of critical utility to examine the faces of a representative selection of joints within each of the joint sets to characterize the crack-face morphology. This will allow us to establish whether a given joint set is composed of extensional (mode I) or shear (mode II or III) cracks. Having the opportunity to examine the faces of cracks that intersect one another will likely allow us to establish the timing of joint development (*e.g.*, Twiss and Moores, 1992).

An independent control on the nature of the joints may be afforded by microscopic examination of vein material in thin section. Where the veins are filled with calcite, the calcite strain-gauge technique can be employed to determine the characteristics of the most recent differential stress field that was sufficient to induce mechanical twinning in calcite (*e.g.*, Groshong, 1972, 1974; Evans and Groshong, 1994). If the calcite twins are bent, information about temperature conditions can be gleaned (Passchier and Trouw, 1998).

The orientation of the joints can now be characterized using spatial statistics pioneered by Fisher (1953) and recently adapted by Cronin (in press, 2006). A minimum of 7 orientation observations would be collected on each joint face to determine the average orientation and the associated uncertainty to a 95% level. Where faults are observed that have shear striae (*i.e.*, slickenlines), the direction of slip can be measured and can also be characterized using Fisher statistics. The result will be a much more robust characterization of the orientation of joints, faults and shear displacements in the area. These techniques were not available when the field work for this thesis project was done.

REFERENCES

Baars, D.L., 1966, Pre-Pennsylvanian paleotectonics--Key to basin evolution and petroleum occurrences in Paradox Basin, Utah and Colorado: American Association of Petroleum Geologists, v. 50, no. 10, p. 2082-2111.

Baars, D.L, and Stevenson, G.M., 1981, Tectonic evolution of the Paradox Basin, Utah and Colorado: Rocky Mountain Association of Geologists Field Conference, Denver, 1981, p. 23-31.

Barbeau, D.L., 2003, A flexural model for the Paradox Basin -- implications for the tectonics of the Ancestral Rocky Mountains: Basin Research, v. 15, no. 1, p. 97-115.

Budnik, R.T., 1986, Left-lateral intraplate deformation along the Ancestral Rocky Mountains -- implications for late Paleozoic plate motions: Tectonophysics, v. 132, p. 195-214.

Cater, F.W., 1960, The salt anticlines of southwestern Colorado and southeastern Utah *in* Geology of the Paradox Basin Fold and Fault Belt: Durango, Colorado, Four Corners Geological Society, 3rd Field Conference, Guidebook, p. 125-131.

Cater, F.W., and Elston, D.P., 1963, Structural development of salt anticlines of Colorado and Utah, *in* Backbone of the Americas: American Association of Petroleum Geologists Memoir 2, p. 152-159.

Craig, L.C., and Cadigan, R.A., 1958, The Morrison and adjacent formations in the Four Corners area *in* Guidebook to the Geology of the Paradox Basin: Salt Lake City, Intermountain Association of Petroleum Geologists, 9th Annual Field Conference, Guidebook, p. 182-192.

Cronin, V.S., 2006, Finding the mean and 95% confidence interval of a set of strike-and-dip or lineation data: Environmental and Engineering Geology, in press.

Dane, C.H., 1935, Geology of the Salt Valley Anticline and adjacent areas - Grand County Utah: U.S. Geological Survey, Bulletin 863, p. 121-124.

Davis, G.H., and Reynolds, S.J., 1996, Structural Geology of Rocks and Regions (2nd ed.): New York, John Wiley, 776 p.

Dickinson, W.R., and Lawton, T.F., 2003, Sequential intercontinental suturing as the ultimate control for Pennsylvanian Ancestral Rocky Mountains deformation: Geology, v. 31, no. 7, p. 4.

Doelling, H.H., 1981, Stratigraphic investigations of Paradox Basin structures as a means of determining the rates and geologic age of salt-induced deformation--A preliminary study: Utah Geological and Mineral Survey Open File Report no. 29, p. 83.

Doelling, H.H., 1982, Geologic studies of the Salt Valley Anticline -- progress report: Utah Geological and Mineral Survey Open-File Report 30, p. 1-24.

_____1983, Observations on Paradox Basin salt Anticlines *in* Grand Junction Geological Society Field Trip: Grand Junction, Colorado, Grand Junction Geological Society, p. 81-90.

_____1985, Geology of Arches National Park: Utah Geological and Mineral Survey, v. 74, p. 15.

_____1988, Geology of Salt Valley Anticline and Arches National Park, Grand County, Utah: Utah Geological and Mineral Survey Bulletin 122, p. 1-58.

_____2000, Geology of Arches National Park, Grand County Utah, *in* Sprinkel, D.A., Chidsey, T.C. Jr., and Anderson, P.B., eds., Geology of Utah's Parks and Monuments: Utah Geological Association Publication 28, p. 11-36.

Elston, D.P., 1960, Early growth of the salt anticlines of the Paradox Basin, Colorado and Utah [abs.]: Geological Society of America Bulletin, v. 71, no. 12, part 2, p. 1858.

Elston, D.P., and Shoemaker, E.M., 1960, Late Paleozoic and early Mesozoic structural history of the Uncompahgre Front, *in* Geology of the Paradox Basin fold and fault belt: Durango, Colorado, Four Corners Geological Society, 3rd Field Conference, Guidebook, p. 47-55.

_____1962, Salt anticlines of the Paradox Basin, Colorado and Utah: Symposium on Salt, 1st, Cleveland, Ohio, 1962, p. 131-146.

Engelder, T., 1993, Stress regimes in the lithosphere: Princeton, New Jersey, Princeton University Press, 457 p.

Evans, M.A., and Groshong, R.H., Jr., 1994, A computer program for the calcite strain-gauge technique: Journal of Structural Geology, v. 16, p. 277-281.

Ferrill, D.A., and Morris, A.P., 2001, Displacement gradient and deformation in normal fault systems: Journal of Structural Geology, v. 23, p. 619-638.

Fisher, R.A., 1953, Dispersion on a sphere: Proceedings of the Royal Society, London, v. A17, pp. 295-305.

Frahme, C.W., and Vaughn, E.B., 1983, Paleozoic geology and seismic stratigraphy of the northern Uncompahgre front, Grand County, Utah, *in* Lowell, J.D. and Gries, R., eds., Rocky Mountain Foreland Basins and Uplifts: Rocky Mountain Association of Geologists, p. 201.

Ge Hongxing, Jackson, M.P.A., Vendeville, B.C., and Hudec, M.R., 1994, Initiation and early growth of salt structures in the Paradox Basin, Utah and Colorado -- insights from dynamically scaled physical experiments [abs.]: American Association of Petroleum Geologists Annual Meeting Abstracts, 1994, p. 154.

Ge Hongxing, Jackson, M.P.A., and Vendeville, B.C., 1996, Extensional origin of breached paradox diapirs, Utah and Colorado -- field observations and scaled physical models: Salt Lake City, Utah Geological Association, Guidebook no. 25, p. 285-293.

Goldstein, A.G., 1981, Comment and reply on 'Plate tectonics of the Ancestral Rocky Mountains': Geology, v. 9, no. 9. p. 387-389.

Groshong, R.H., Jr., 1972, Strain calculated from twinning in calcite: Geological Society of America Bulletin, v. 82, p. 2025-2038.

Groshong, R.H., Jr., 1974, Experimental test of the least-squares strain gauge calculation using twinned calcite: Geological Society of America Bulletin, v. 85, p. 1855-1864.

Heyman, G.O., 1983, Distribution and structural geometry of faults and folds along the northwestern Uncompahgre Uplift, western Colorado and eastern Utah: Grand Junction, Colorado, Grand Junction Geological Society, Field Trip Guidebook, p. 45-57.

Hintze, L. F., 1988, Geologic history of Utah: Brigham Young University, Geology Studies, Special Publication 7, p. 202.

Hobbs, B.E., Means, W.D., and Williams, P.F., 1976, An outline of structural geology: New York, John Wiley & Sons, 571 p.

Huffman, C.A., Jr., 1992, Late Paleozoic depositional controls in the Paradox Basin, Colorado and Utah: Geological Society of America, Abstracts with Programs, v. 24, no. 7, p. 31.

Jackson, M.P.A., and Vendeville, B.C. 1994, Initiation of salt diapirism by regional extension—global setting, structural style, and mechanical models: Austin, Texas, Bureau of Economic Geology, Report of Investigations no. 215, p. 25.

Jones, R.W., 1959, Origin of salt anticlines of the Paradox Basin: American Association of Petroleum Geologists Bulletin, v. 43, no. 8, p. 1869-1895.

Kattenhorn, S.A., and Pollard, D.D., 2001, Integrating 3-D seismic data, field analogs, and mechanical models in the analysis of segmented normal faults in the Wytch Farm oil field, southern England, United Kingdom: American Association of Petroleum Geologists Bulletin, v. 85, no. 7, p. 1183-1210.

Kitcho, C.A., 1981, Characteristics of surface faults in the Paradox Basin: Durango, Colorado, Rocky Mountain Association of Geologists, Field Conference Guidebook, p. 1-22.

Kluth, C. F., 1998, Late Paleozoic deformation of interior North America--The Greater Ancestral Rocky Mountains: American Association of Petroleum Geologists Bulletin, vol. 82, p. 2272-2276.

_____2000, The greater ancestral Rocky Mountains--Summary and suggestions for the path forward [abs.]: Geological Society of America, v. 32, no.7, p. 467.

Kluth, C.F., and Coney, P.J., 1981, Plate tectonics of the Ancestral Rocky Mountains: Geology, v. 9, p. 10-15.

Larsen, P., 1988, Relay structures in a lower Permian basement-involved extension system, East Greenland: Journal of Structural Geology, v.10, no.1, p. 3-8.

Maune, D.F., 2001, Digital elevation model technologies and applications -- The DEM users manual: Bethesda, Maryland, American Society for Photogrammetry and Remote Sensing, 539 p.

Molenaar, C.M., 1981, Mesozoic stratigraphy of the Paradox Basin -- an overview: Denver, Colorado, Rocky Mountain Association of Geologists, Field Conference, Guidebook, p. 119-127.

Ohlen, H.R., and McIntyre, L.B., 1965, Stratigraphy and tectonic features of the Paradox Basin, Four Corners Area: American Association of Petroleum Geologists Bulletin, v. 49, no. 11, p. 2020-2040.

Passchier, C.W., and Trouw, R.A.J., 1998, Microtectonics: Berlin, Springer, 289 p.

Peacock, D.C.P., and Parfitt, E.A., 2002, Active relay ramps and normal fault propagation on Kilauea Volcano, Hawaii: Journal of Structural Geology, v. 24, p. 729-742.

Peacock, D.C.P., and Sanderson, D.J., 1990, Displacements, segment linkage and relay ramps in normal fault zones: Journal of Structural Geology, v. 15, no. 6, p. 721-733.

_____1991, Displacements, segment linkage and relay ramps in normal fault zones: Journal of Structural Geology. v. 13. no. 6, p. 721-733.

_____1994, Geometry and development of relay ramps in normal fault systems: American Association of Petroleum Geologists Bulletin, v. 78, no. 2, p. 147-165.

Stokes, W.L., 1986, Geology of Utah: Utah Geological and Mineral Survey, 1986, Salt Lake City, 280 p.

Suppe, J., 1985, Principles of structural geology: Englewood Cliffs, New Jersey, Prentice-Hall, Inc., 537 p.

Szabo, E., and Wengerd, S.A., 1975, Stratigraphy and tectogenesis of the Paradox Basin *in* Canyonlands: Durango, Colorado, Four Corners Geological Society, 8th Field Conference Guidebook, p. 193.

Trudgill, B., and Cartwright, J., 1994, Relay-ramp forms and normal-fault linkages, Canyonlands National Park, Utah: Geological Society of America Bulletin, v. 106, p. 1143-1157.

Twiss, R.J., and Moores, E.M., 1992, Structural geology: New York, W.H. Freeman and Company, p. 43-48.

Vendeville, B.C. and Jackson, M.P.A., 1992a, The rise of diapirs during thin-skinned extension: Marine and Petroleum Geology, v. 9, no. 4, p. 331-353.

_____1992b, The rise and fall of diapirs during thin-skinned extension: Bureau of Economic Geology, Report of Investigations no. 209, The University of Texas at Austin, p. 60.

Warner, L.A., 1983, Comment and reply on 'Plate tectonics of the Ancestral Rocky Mountains': Geology, v. 11, no. 2, p. 120.

Wengerd, S.A., and Strickland, J.W., 1954, Pennsylvanian stratigraphy of the Paradox Salt Basin, Four Corners Region, Colorado and Utah: American Association of Petroleum Geologists Bulletin, v. 38, no. 10, p. 2157-2199.

Wheeler, R.L. and Holland, S.M., 1978, Style elements of systematic joints--An analytical procedure with a field example *in* Proceedings of the Third International Conference on Basement Tectonics, 3rd, Durango, Colo., 1978: Basement Tectonics Committee Publication, no. 3, O'Leary, D.W. and Earle, J.L., eds., p. 393-404.

Withjack, M.O. and Scheiner, C., 1982, Fault patterns associated with domes--An experimental and analytical study: American Association of Petroleum Geologists Bulletin, v. 66, no. 3, p. 302-316.

Woodward-Clyde Consultants, 1983, Overview of the regional geology of the Paradox Basin study region: Battelle Memorial Institute, Office of Nuclear Waste Isolation technical report, 433 p.

Ye Hongzhuan, Royden, L., Burchfiel, B.C., and Schuepbach, M., 1996, Late Paleozoic deformation of interior North America -- the greater Ancestral Rocky Mountains: American Association of Petroleum Geologists Bulletin, v. 80, no. 9, p. 1397-1432.

PLATES

PLATE I

Aerial Photograph Collage

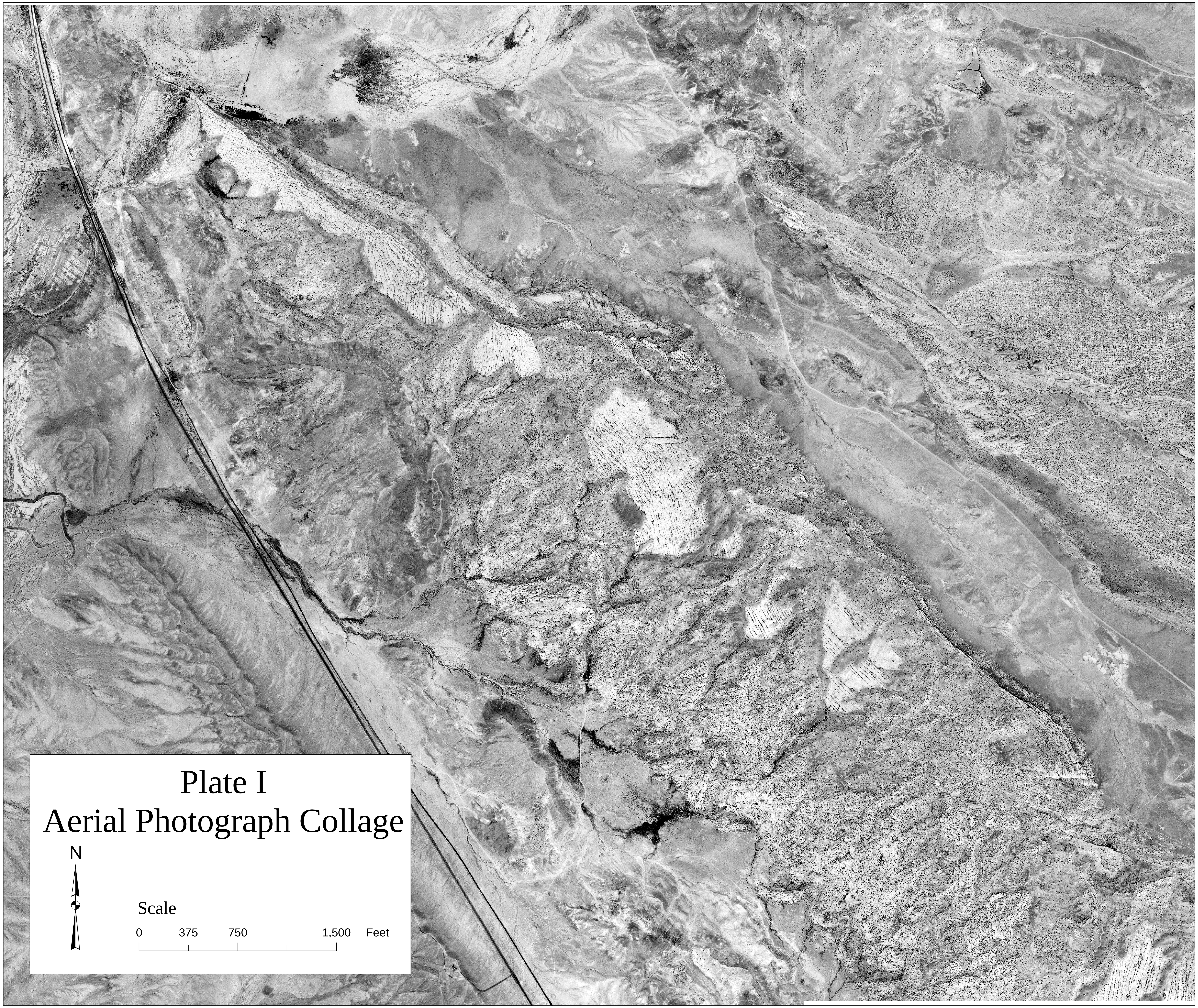

Plate I
Aerial Photograph Collage

PLATE II

Geologic Map

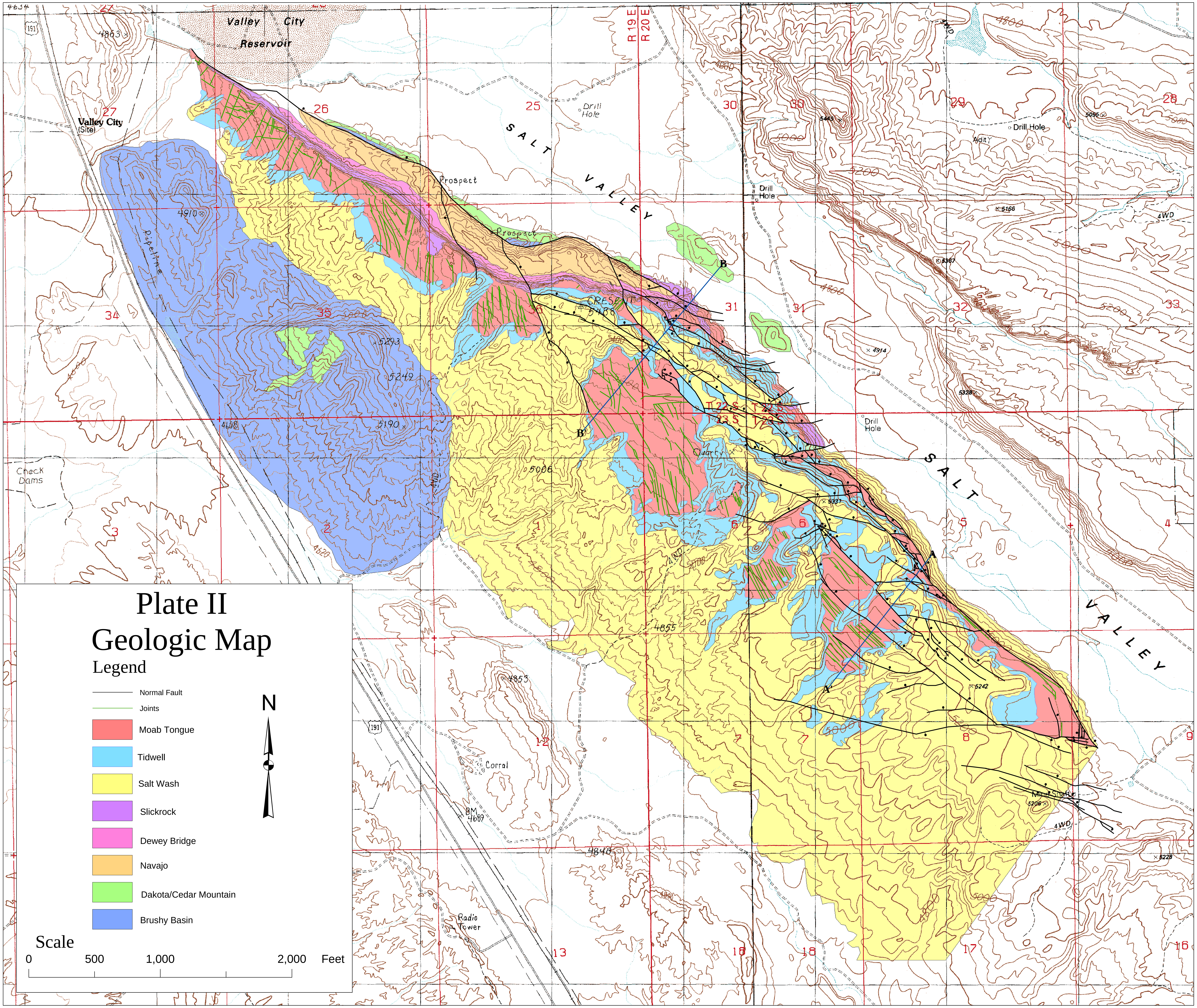

Plate II
Geologic Map
Legend
Normal Fault
Joints
Moab Tongue
Tidwell
Salt Wash
Slickrock
Dewey Bridge
Navajo
Dakota/Cedar Mountain
Brushy Basin
N
Scale
0
500
1,000
2,000
Feet
Valley City
Reservoir
Valley City
(Site)
SALT VALLEY
SALT VALLEY
SALT VALLEY
Prospect
Prospect
Drill Hole
Drill Hole
Drill Hole
Adit
Quarry
Pipeline
Check Dams
Corral
Radio Tower
R 19 E
R 20 E